UNIVERSITY OF OKLAHOMA

GRADUATE COLLEGE

EXPERIMENTAL INVESTIGATION OF POLYMER-BASED LOST CIRCULATION MATERIALS FOR FLUID LOSS TREATMENT UNDER HIGH TEMPERATURE USING ADDITIVE MANUFACTURING.

A THESIS

SUBMITTED TO THE GRADUATE FACULTY

In partial fulfillment of the requirements for the

Degree of

MASTER OF SCIENCE

By

TOBENNA VICTOR ANYAEZU

Norman, Oklahoma

2023

EXPERIMENTAL INVESTIGATION OF POLYMER-BASED LOST CIRCULATION MATERIALS FOR FLUID LOSS TREATMENT UNDER HIGH TEMPERATURE USING ADDITIVE MANUFACTURING.

A THESIS APPROVED FOR THE MEWBOURNE SCHOOL OF PETROLEUM AND GEOLOGICAL ENGINEERING

BY THE COMMITTEE CONSISTING OF

Dr. Saeed Salehi, Chair

Dr. Ramadan Ahmed

Dr. Hamidreza Karami

Acknowledgment

I sincerely thank my thesis supervisor, Dr. Saeed Salehi, for taking me under his wing and supporting me through this journey for the past three years. From the first day, I walked into the lab, his unwavering support, guidance, and constant support have been monumental. I will forever be indebted to him for pushing me and helping me achieve my research goals.

I would be remiss not to thank my committee members for their time and effort. I am truly honored to have Dr. Ramadan Ahmed and Dr. Hamidreza Karami as my thesis committee members. The wealth of knowledge they brought into this research is unquantifiable.

Also, I am immensely grateful to the University of Oklahoma, including the Mewbourne School of Petroleum and Geological Engineering (MPGE), for their financial support throughout my master's education. I am also grateful to the Department of Energy (DOE) and Qatar National Research Fund (QNRF) for partial financial support for this thesis work.

I am also grateful to the Lab manager at the Well Construction Technology Center, Jeff McCaskill. He provided me access to the research materials and equipment. His technical knowledge and know-how were invaluable as I navigated research complexities and ran experiments.

I would also like to thank my research fellows, including Cesar Vivas, Dr. Musaab Magzoub, and Dr. Mohammed AbdelMjeed, for their valuable input and guidance while running multiple experiments. Indeed, I could not have accomplished all of this without them.

Finally, I would like to thank my friends, including Jasmin Sneed, Michael Olubode, Judah Odiachi, Chinedu Nwosu, and Chinedu Nsude, my sister and brother-in-law, Chisom and Nonso Olikagu for being there in my lows and highs. They have been my backbone these past years. Also, plenty of thanks goes to God, my lovely and supportive parents, and my siblings.

Table of Contents

List of Figures

List of Tables

Abstract

Lost circulation continues to be one of the most troublesome problems encountered during drilling. The financial cost of lost circulation in geothermal drilling can rise to 15% of the total drilling cost. A corrective approach to preventing lost circulation is using lost circulation materials (LCMs) to plug the fractures in the wellbore, minimizing fluid loss and strengthening the wellbore. The overall objective of this research is to test potential LCMs for sealing fractures under high-temperature conditions.

This research assessed the concept of recreating complex and drilling-induced fractures using 3D printing. This study aims to generate fractures that look closer to the ones present downhole in geothermal wells. Two LCMs, shape memory polymer (SMP) and crosslinked polymer, were investigated for their potential to reduce fluid loss and seal complex fractures. Experimental investigations, such as particle size distribution, rheology, gelation kinetics, alkalinity control, and fracture sealing tests, were conducted to optimize the concentration of LCMs in drilling mud. The experiments were conducted at temperatures between 93.3°C(200°F) to 150°C(302°F).

The results included the optimum concentration of SMP that can seal complex fracture zones. Compared to walnuts, a conventional LCM, SMP significantly reduced mud loss. Additionally, the importance of particle size distribution in the performance of granular LCMs is highlighted. Rheology and gelation kinetics are essential for the settable crosslinked polymer in any successful field application. This study's novelty is using a 3D printed fracture disc for testing and optimizing SMP and crosslinked polymer, which should reduce lost circulation in high-temperature environments.

Chapter 1 : Introduction

1.1 Overview of Lost Circulation in High-Temperature Formations

Lost circulation is one of the most common oil and geothermal drilling problems. Losing costly drilling fluid to the formation and the non-productive time (NPT) spent recovering circulation increases the total well expenses by 10 – 25% (Allahvirdizadeh, 2020). The consequences of leaving this problem unattended may lead to other wellbore instability problems, such as differential sticking, poor hole cleaning, well control issues, and packoffs. This problem has persisted in the oil, gas, and geothermal industries. Mud losses to the formation often worsen as the depth increases, causing the wellbore to be increasingly unstable, affecting wellbore cleaning and reducing the rate of penetration (ROP). Most lost circulation incidents occur at the wellbore surface, then can extend deep into the formation.

Lost circulation occurs during geothermal drilling because geothermal wells are mainly drilled in volcanic and hard formations, with natural fracture apertures often greater than 1000 microns. This factor and harsh drilling environments from under-pressurization in fractured and altered material zones make lost circulation more common in geothermal wells than in oil wells (Saleh et al., 2020). A study in Iceland revealed lost circulation to be the primary cause of wellbore instability in 75% of the wells in the Hengill Geothermal Area (Sveinbjornsson & Thorhallsson, 2014). These problems often led to cement losses during cementing operations. In the United States alone, loss of drilling fluid to the formations make up roughly 10% of well costs in brown geothermal fields and nearly 20% in green geothermal wells (Finger and Blankenship, 2010).

The key to understanding lost circulation requires knowledge of the formation's mechanical and elastic properties, including pore pressure, Poisson's ratio, near-wellbore stresses, and the physical and chemical properties of the drilling mud (Feng & Gray, 2016). Mitigating circulation

loss involves prevention and remediation approaches, as shown in Figure 1. Prevention includes following best drilling practices, selecting the proper fluid when drilling a particular hole section, and pretreating the drilling fluid with select wellbore strengthening materials (WSMs).

Best drilling practices include maintaining the right mud weight between the hydrostatic and formation breakdown pressure, which is essential in preventing losses in the formation. Drilling fluid selection, the other part of prevention, involves selecting the appropriate drilling mud for each well section. Suppose knowledge of the environment is known before drilling and fracture zones are anticipated; the drilling mud can be pretreated with wellbore strengthening materials, including fine graphite and calcium carbonate ($CaCO_3$). Pretreating the drilling fluid with selected WSMs before drilling known high-risk formations can be invaluable to the success of drilling operations (Whitfill & Wang, 2005). Wellbore strengthening has been applied successfully in formations with varying fracture gradients and narrow mud window (Kiran et al., 2017; Salehi & Nygaard, 2011).

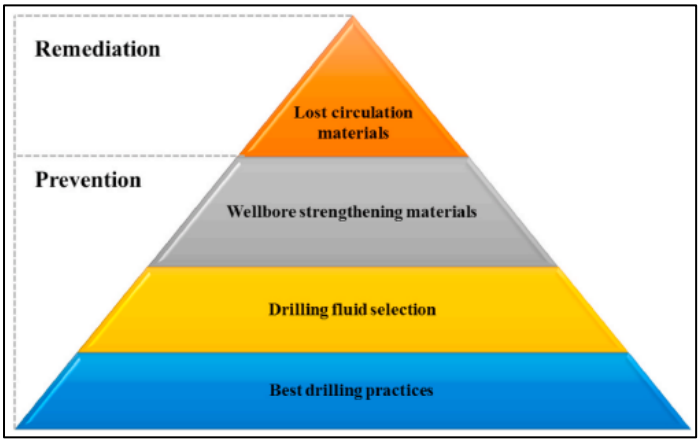

Figure 1.1: Steps showing approaches to combating lost circulation (Cook et al., 2012)

Corrective approaches to lost circulation only treat the drilling fluid after a loss has occurred (Magzoub et al., 2021). The lost circulation material is added to the drilling mud continuously or intermittently as a spotted pill. Lost circulation materials for curing mud losses

include cotton hulls, micronized cellulose, and fiber (Vivas & Salehi, 2022). A combination of multiple methods often yields the best results (Cook et al., 2011; Ghalambor et al., 2014).

1.2 Problem statement and motivation

Lost circulation is a costly problem, especially in high-temperature oil and geothermal wells. Loss of drilling fluid often leads to other drilling problems, such as stuck pipes, kicks, and blowouts. The depth of the wellbore, bottom-hole temperature, and the size of the fracture often limits the selection of proper treatment. Examples of formations susceptible to lost circulation include naturally fractured formations, highly permeable rocks, and depleted reservoirs.

Multiple lost circulation materials (LCM) have been developed over the years, including polymer gels, smart LCMs, and micronized cellulose. However, there is a gap in the testing and developing LCMs for large fractures in high-temperature zones. Innovation in testing LCMs has somewhat stalled over the years.

The motivation of this study includes the application of additive manufacturing that closely represents natural fractures as seen in geothermal wells. Also, novel lost circulation materials not previously used in geothermal applications are introduced. Therefore, improving the formulation and testing of LCMs capable of effectively bridging and sealing fracture zones is highly beneficial to the geothermal and petroleum industry.

1.3 Research Objectives

This study investigates the application of additive manufacturing (3D printing) in testing potential lost circulation materials (LCMs) capable of sealing large fractures in high-temperature formations. Shape memory polymer (SMP), polymer gel, and walnut are considered.

The research objectives for this study are summarized below:

1. Design 3D printed fracture disc with representative fracture orientation as found in geothermal wells.
2. Investigate the effects of the LCM concentration in bridging and sealing the 3D printed disc at 200°F (93.3°C). The weight concentration varies between 1% and 5%.
3. Investigate the rheological properties of the PAM (Polyacrylamide)/PEI (Polyethyleneimine) polymer mud at 302°F (150°C).
4. Study the gelation kinetics of PAM and PEI gel.
5. Examine the efficiency and optimum concentration of PAM/PEI polymer mud for plugging deep tapered fractures in the wellbore during drilling.

1.4 Research Outline and Scope of Study

The research methodology for this study is divided into 3 parts to cover the scope and fulfill the objectives. The parts include reviewing existing literature, experimental investigation, and research data analysis.

The scope of each part of this research is discussed below:

I. Theoretical review: A thorough literature review on drilling fluid functions and how it relates to lost circulation is presented. Published books, journal articles, and conference proceedings were reviewed during this study. An in-depth understanding of the two LCMs investigated in this study, Shape memory polymer (SMP) and Polyacrylamide/Polyethyleneimine (PAM/PEI) polymer system, are presented. Gaps were identified in the current use of LCMs in high-temperature wells. The review outcome provided a base for integrating the experimental methods and achieving the objectives.

II. Experimental investigation: The laboratory methods used in this study include designing and printing 3D fracture discs, drilling fluid formulation, rheological measurements,

particle size distribution, and permeability plugging tests. The goal was to design and optimize lost circulation materials and settable systems for high-temperature environments.

III. Research Data Analysis: After the experimental investigation, the results from the particle size distribution, rheology, and filtration experiments are analyzed. The in-depth analysis provided insights into evaluating the performance of each lost circulation material tested.

Chapter 2 : Literature Review

This chapter introduces the essential functions of the drilling fluid and how improper drilling conditions can lead to mud losses and, thus, lost circulation. A comprehensive study of the causes and remedies of lost circulation is presented. An extensive review of two kinds of lost circulation materials (LCMs) used in the study, shape memory polymers (SMPs) and crosslinked polymer mud, is detailed. The limitations and challenges in developing and testing lost circulation materials for high-temperature environments are highlighted.

2.1 Review of Drilling Mud and Losses to The Formation

Drilling mud is the fluid system that comprises a volume of fluid pumped with unique mud pumps from the surface, through the drill string, and out the nozzles of the drill bit; this mud goes up the annulus in the wellbore and back to the surface, for removing solids and maintenance treatment. The drilling mud is the only component that remains in contact with the wellbore throughout the process.

The drilling mud is designed to perform the following functions:

1. Cool and lubricate the drill string and bit.
2. Clean the wellbore by transporting the drilled cuttings (rock fragments) from the bottom to the surface, where it is mechanically removed.
3. Balances formation pressure in the wellbore to minimize well control problems
4. Prevents and minimizes damage to productive formations
5. Transmit hydraulic horsepower to the drill bit.
6. Assist in drilling mud telemetry.

Critical properties must be optimized and monitored during the drilling process for the drilling mud to perform its desired functions. The main properties of the drilling mud are:

- density
- rheological properties, including viscosity, gel strength, and yield stress
- fluid loss and filtration properties
- mud stability at high temperatures and pressure

The cost of the drilling mud can average 10% of the total drilling cost; however, the performance of the drilling mud can affect the overall drilling cost in multiple ways. A well-designed and well-maintained drilling mud can help achieve cost savings throughout the drilling process by enhancing the rate of penetration (ROP) (Sharma et al., 2021). If the drilling mud is poorly designed or maintained, it could lead to improper drilling conditions and potentially lost circulation.

Lost circulation is the uncontrollable loss of drilling mud into the formation, sometimes called the thief zone. Lost circulation can be partial or total; mud can flow to the surface with mud losses into the formation, or all mud can be lost entirely to the formation where no drilling mud returns to the surface.

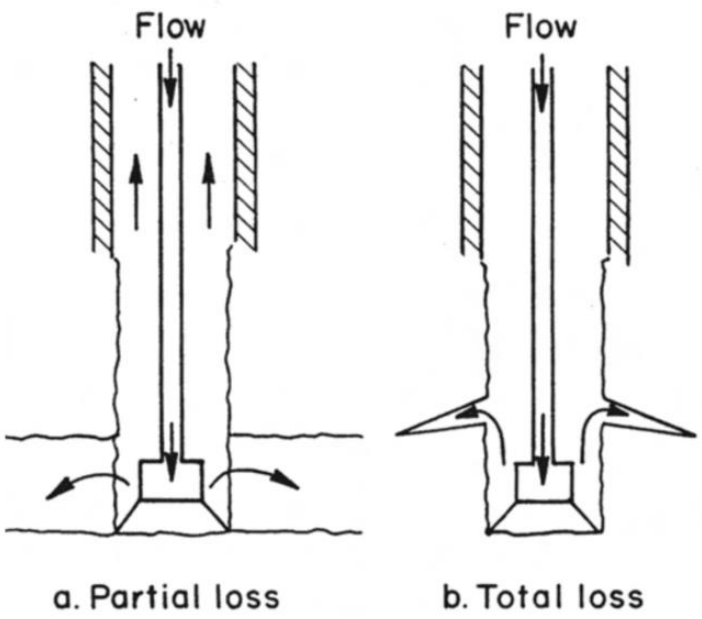

Figure 2.1: Lost circulation zones (Lake, 2006)

Rock formations that are naturally fractured, cavernous, and have high permeability are potential zones for lost circulation. Additionally, improper drilling factors and conditions can lead to induced fractures, creating lost circulation zones. Factors that lead to induced fractures in formations include excessive downhole wellbore pressure and setting intermediate casing too high in transition zones.

Excessive wellbore pressures are usually caused by high annular-friction pressure loss, high flow rates, and tripping in too swiftly, resulting in high surge pressure (Olubode et al., 2022a). These factors lead to an increase in the mud equivalent circulating density (ECD). ECD is the effective density of the drilling mud in the wellbore. ECD results from the sum effects of the hydrostatic pressure imposed by the static drilling fluid column and the frictional pressure in the wall of the wellbore (Raabe & Jortner, 2022).

$$ECD = \frac{(MW + AFP)}{C * TVD} \quad 2.1$$

where,

ECD = Equivalent Circulating Density (ppg)

MW = Mud Weight (ppg)

AFP = Annular Frictional Pressures in the annulus (psi)

TVD = True Vertical Depth (ft)

C = Conversion factor = 0.052

In addition, to increase ECD, improper annular wellbore cleaning, excessive drilling mud weight, and shutting a well in high-pressure shallow gas formation can induce fractures, which leads to lost circulation. Equation 2.2 and 2.3 conditions must be maintained to avoid induced fracturing during drilling and tripping.

$$ECD = MW + AFP < FFP \quad (2.2)$$

$$ECD = MW + SP < FFP \quad (2.3)$$

where,

FFP = formation fracture pressure in PPG

SP = Surge pressure

As drilling mud flows in the wellbore, it absorbs heat from the formation, increasing its temperature. The increase in temperature and pressure has a significant effect on the ECD. Harris and Osisanya (2005) conducted a simulation to determine the effects of temperature and pressure on ECD. The authors found that the decrease in density due to thermal expansion is more prominent than the increase in density due to temperature. Thus, the net effect of increased temperature and pressure in the wellbore is a decrease in mud ECD.

The ECD needs to be kept within a specific window. The lower bound of the mud window/ wellbore pressure is usually set at the formation pressure, and the upper bound of the wellbore pressure profile is the formation fracture pressure. If the wellbore pressure falls below the formation pressure, an inflow of formation fluids called "kick" may occur. Similarly, if the wellbore pressure goes above the formation fracture pressure, the formation could get fractured, and drilling mud could get lost into the formation (lost circulation).

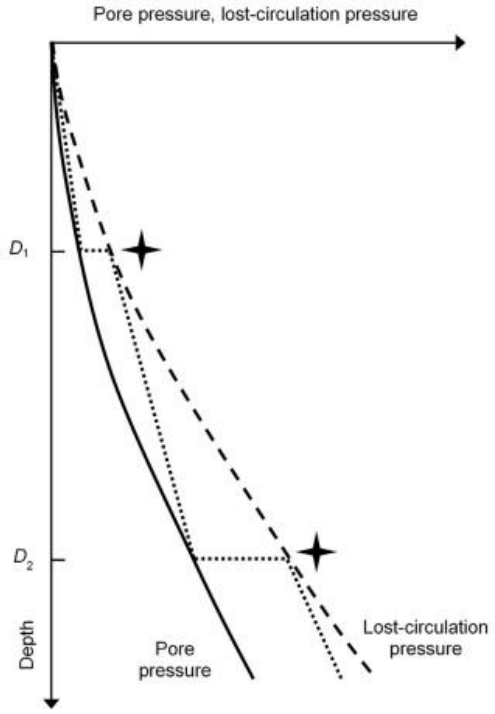

Figure 2.2: Pore pressure and lost circulation pressure profile along the depth of the well (Lavrov, 2016)

When lost circulation happens, some of the drilling fluid is lost to the rock formation. The economic impact of lost circulation includes the costs of the lost drilling mud and nonproductive time (NPT) spent trying to regain mud circulation. The total cost of lost circulation can amount between 10% - 25% of the total drilling. In addition to the economic cost, lost circulation may cause additional drilling problems, including poor hole cleaning, improper cuttings transport, and differential sticking. Severe cases of lost circulation may lead to well control issues as the drilling

mud column may not be sufficient to withstand the formation pressure. This underbalanced pressure may eventually lead to the influx of formation fluid into the wellbore, resulting in a kick or borehole collapse (Abdollahi et al., 2004).

Lost circulation is also common in geothermal drilling. Fracture sizes in geothermal formations are usually substantial, which leads to severe or total lost circulation. Lost circulation problems may often lead to cement losses in the formation during well cementing. In the Hengill Geothermal Area in Iceland, it was revealed that 18 of the 24 wells suffered from lost circulation or wellbore collapse as the primary drilling problems (Sveinbjornsson et al., 2014). Wells drilled in formations with high geothermal gradients are more prone to mud losses caused by cooling. When the cold drilling mud meets the hotter formation in the wellbore, rock contracts, and hoop stress around the wellbore becomes smaller. Thus, the rock becomes easier to fracture. (Tare et al., 2001).

The most straightforward way to prevent lost circulation is to keep the downhole pressure in the drilling mud window below the fracture pressure and above the formation hydrostatic pressure. However, this approach has often proved futile because of the uncertainty in determining the formation fracture pressure in formations with complex pore pressure and stress distributions. In naturally fractured rocks, fracture sizes are usually large, and the orientation is complex. Different fracture orientation translates to fractures having multiple sizes, orientations, losses, and wellbore pressure. Since no single fracture pressure exists, the values obtained from formation integrity and leak-off tests become unreliable.

Drilling records, well logs, and mineralogy analysis can help in the decision-making approach to mitigating lost circulation. Winn et al. (2023) examined the drilling records from 4 geothermal fields in the US – McGinness Hills in central Nevada, Steamboat Hills and Don A.

Campbell in western Nevada, and Puna Geothermal Venture in Hawaii- to identify the most prone lost circulation zones. Partial lost circulation events occurred for some wells at 0 – 450 m. On the other hand, total lost circulation with no drilling fluid return to the surface occurred at a depth greater than 700 m. Most lost circulation events occurred at faults intersections, excluding Puna, where no faults were detected in the 3D geologic model. Observation of some secondary minerals, including hyaloclastite, was also associated with lost circulation events in the Puna fields (Spielman et al., 2006; Rickard et al., 2011).

Mitigating lost circulation in the formations above the reservoir was accomplished using conventional LCMs first, before proprietary blended LCMs, in the order of least expensive. Alternatively, Lowry et al. (2022) recommended that addressing lost circulation with more advanced and expensive LCMs can save drilling time. Conventional LCMs used in the 4 geothermal fields include shells, walnut pellets, fiber, and micronized cellulose, while proprietary blended LCMs include PrimaSeal™, Kwik-Seal™, and CHEK-LOSS™. In the productive zone, aerated drilling mud is considered the prima option in sealing lost zones to minimize formation damage and loss of reservoir productivity. Occasionally, the productive formation may be drilled blindly with no drilling fluid.

Combatting lost circulation is a complex problem that requires a multidisciplinary approach; this includes knowledge of rock mechanics, drilling fluid rheology, well planning and optimization of loss circulation materials, and drilling hydraulics (Whitfill & Hemphill, 2003). Difficult drilling conditions, like high-temperature, high-pressure wells, make accessing reserves in different parts of the world even harder.

2.2 Mechanisms and Diagnostics of Lost Circulation

Diagnosing lost circulation at the well site involves monitoring the pit level and mud loss flow rate. The mud "pit" is a steel tank that holds the drilling mud during drilling. Mud pits are used to suction the mud pumps and settle and store mud sediments (Olubode et al., 2022b). Monitoring the mud pit using acoustic or floating sensors can provide the cumulative volume of drilling mud lost over time. A drop in the mud-pit level can indicate loss of circulation. The mud loss flow rate is defined as the difference in the flow rate of the drilling mud going into the well and the flow rate of the drilling mud leaving the well. The mud loss flow is measured with a flow meter at the well site. Drilling mud losses can be categorized based on severity (loss rate).

- seepage losses (less than 10 bbl/h)
- partial losses (10 – 100 bbl/h)
- severe losses (greater than 100 bbl/h)
- total losses (no mud return to the surface)

It is essential to know that seepage losses occur more often in high porosity, high permeability sedimentary rocks such as sandstone and siltstone. Partial losses are more associated with unconsolidated sand and gravel. Similarly, partial losses are also expected in natural and induced fractures. Severe losses happen in unconsolidated sandstones, gravels, and highly fractured geothermal hard rocks. Total losses are often associated with vuggy and cavernous formations and fracture systems with large fracture openings.

Classification of mud losses based on severity/loss rate and mud pit level, although simplistic, can often be misleading as it does not account for the origin of the loss or mechanism. Based on origin, mud losses are ascribed to:

- porous matrix
- large cavities (vugs)
- natural fractures
- drilling-induced fractures

These mechanisms, including mud losses in severe environments, are expanded below.

2.2.1 Mud losses in high porosity and permeability matrix

Mud losses in porous matrix occur when a high permeability and porosity matrix meets the drilling fluid. The onset of the mud losses is gradual, and the fluid loss rate increases with time as more rock matrices are exposed. Then, the filter cake builds up gradually, and the loss rate decreases. The mud loss signature and variation of the pit level with time are shown in the figure below.

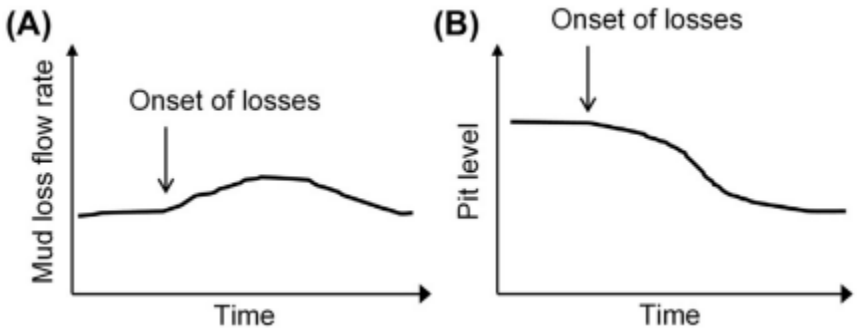

Figure 2.3: (A) Mud loss rate versus time for a high porosity and permeability rock matrix (B) and the variation in pit level with time

Examples of mud losses in high porosity and permeability matrix include losses in unconsolidated sandstone, gravel, and defragment rocks.

2.2.2 Mud losses in Large Cavities and Vugular formations

Cavities and vugs are found in carbonates and are subjected to dissolution from fluid over geologic time. Vugs are usually lined with minerals such as quartz and calcite. The size of the vugs varies

from small to medium. Large cavities and vugs are associated with carbonates rock such as limestones and dolomites.

Mud losses start suddenly when the drill bit and mud come in contact with vugs and large cavities. The volume of drilling mud losses can be large and sudden. The mud loss signature and variation of the pit level with time are shown in the figure below.

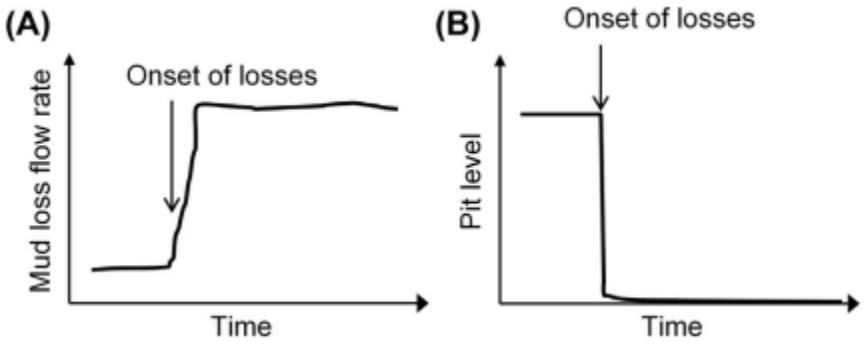

Figure 2.4: (A) Mud loss rate versus time for a large cavity and Vugular formations (B) and the variation in pit level with time

2.2.3 Mud losses in natural fractures

Natural preexisting fracture networks in rock formations can become pathways and the origin of loss circulation. Factors that control mud losses in natural fracture networks depend on the following:

- wellbore pressure
- fracture size or opening
- composition and rheology of the drilling mud
- filter cake build-up

If the fracture openings are large enough and well connected, mud losses can be severe and total. Natural fractures are common in some shale reservoirs and can enhance effective permeability. Mud losses in natural fractures typically start with a sudden drop in the mud flow

rate out of the wellbore. The drilling mud flow rate versus time shows a sudden increase and a gradual drop in the differential mudflow, as shown in Figure 2.5.

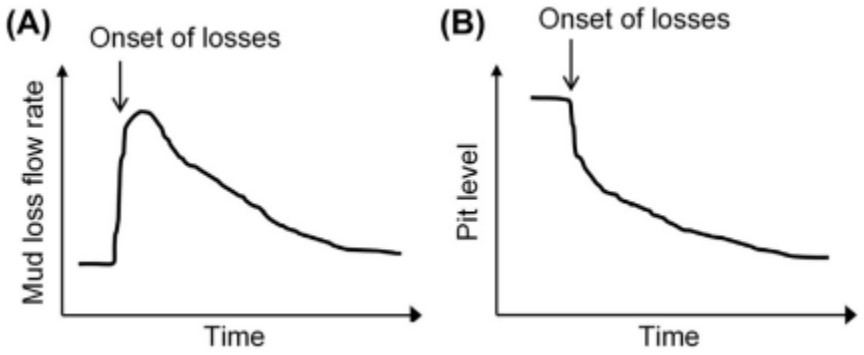

Figure 2.5: (A) Mud loss rate versus time for natural fractures (B) and the variation in pit level with time

The two significant factors in controlling the effects of the opening of the natural fracture are the fracture aperture and bottom hole wellbore pressure. Initially, natural fractures can be either open or closed (Zhou et al., 2022). As part of the drilling process, the wellbore pressure can be sufficient to reopen the fracture further. As the reopening process continues, the fracture aperture increases, and the mud losses in the fracture increase with the fracture permeability. Figure 2.6 below demonstrates this process.

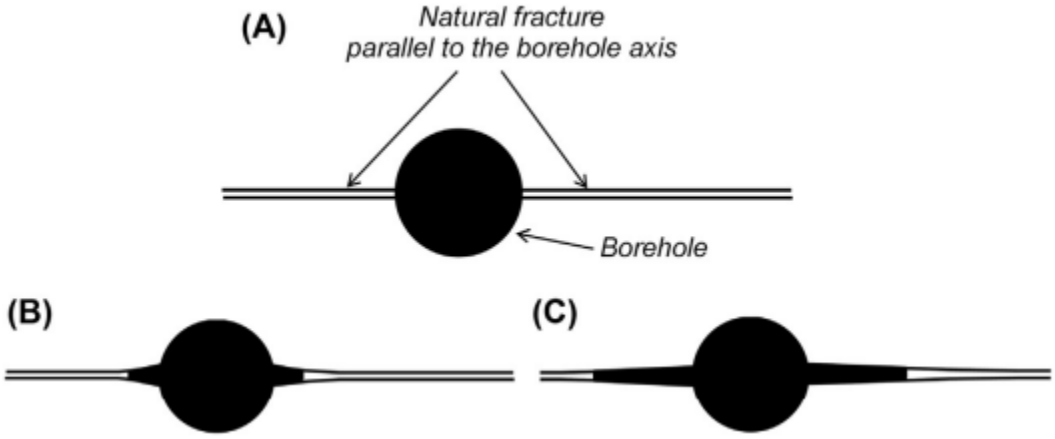

Figure 2.6: Reopening of natural fractures (A) initial state of fracture before opening (B) reopening of the fracture and beginning of mud losses into the fracture (C) drilling mud continues entering and reopening the fracture farther away from the wellbore. (Lavrov, 2016)

2.2.4 Mud losses in drilling-induced fractures

Rock formations can get fractured when the bottom hole well pressure exceeds the fracturing pressure. The fracturing pressure depends on the minimum in-situ pressure, and the fracture is created along the path of least resistance. The fracture pressure is estimated from formation integrity tests, including leak-off tests (LOT), extended leak-off tests (XLOT), and Diagnostics Fracture Injection Testing (DFIT). The wellbore pressure must exceed the formation breakdown pressure (FBP) upon fracture initiation. FBP is the wellbore pressure at which the drilling mud enters the initiated fracture, leading to fracture propagation. An induced fracture differs from a natural one because it has little to no initial aperture. Upon fracture initiation, the drilling mud continues to invade the fracture, and the fracture width grows more extensive, as demonstrated in Figures 2.7 and 2.8.

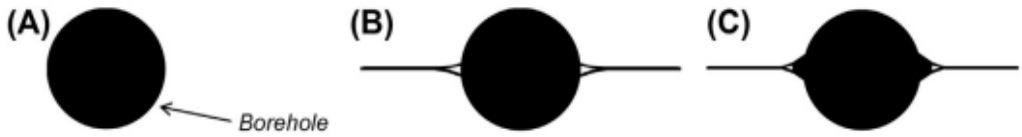

Figure 2.7: Initiation of a drilling-induced fracture: (A) before Initiation; (B) after the fracture has opened but mud invasion; (C) the fracture has opened and mud invasion in the fractured body.

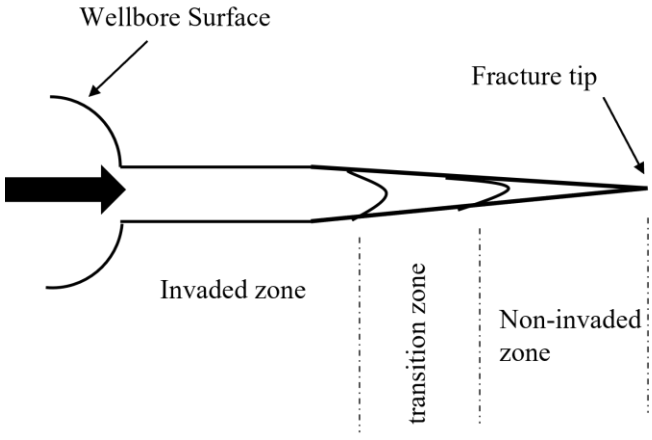

Figure 2.8: The three zones in a drilling-induced fracture. The arrow shows the direction of the mud flow and fracture propagation.

As the drilling mud continues to invade the fracture tip and body, this process creates multiple zones, including the invaded, transition, and noninvaded zone. How large the fracture can grow depends on the fracture aperture, rheology, and solid content of the drilling mud. It is important to note that the thickness of the filter cake formed on the wellbore surface affects the length of the fracture. Also, the length of the noninvaded zone increases with the young's modulus of the rock.

Loss of circulation from drilling-induced fractures is commonly encountered while drilling, cementing, and tripping. This problem has been associated with inappropriate mud windows (Ghalambor et al., 2014). Lack of geological information and incorrect prediction of the mud weight window are some of the causes of wellbore stability issues during drilling. (Salehi and Nygaard, 2012; Mannon and Salehi, 2012)

2.2.5 Lost Circulation in High-Temperature Geothermal Wells

Lost circulation in high-pressure, high-temperature wells is aggravated due to the following factors:

- high-temperature wells have small or reduced drilling margins.
- thermal degradation of drilling mud properties at elevated temperatures.
- geothermal formations such as granite and basalt have natural fractures of large aperture.

In high-temperature formations, the thermal degradation of drilling muds makes the mud lose its solid retention properties and reduces viscosity and cuttings carrying properties. This creates variation in the density of the mud along the well path and can lead to barite sagging and settling in the annulus. Natural fractures are paths of least resistance for drilling mud to invade the formation, as explained in section 2.2.3. Although the large fracture sizes of geothermal formations

are a positive factor in the commerciality of geothermal ventures, they often cause severe or total lost circulation during drilling. Low pore pressure in geothermal formations also means a massive overbalance during drilling.

2.3 Review of Current Solutions Applied to Lost Circulation

Preventing lost circulation is cheaper and more expensive than curing mud losses. Several solutions to prevent and cure lost circulation include plugging materials in a single lost circulation treatment, combining multiple lost circulation materials, wellbore strengthening, cementing, and casing while drilling approaches. Two categories exist for lost circulation solutions; remedial treatment if lost circulation is anticipated and preventive treatment if lost circulation suddenly happens.

2.3.1 Preventive Approach

Preventing lost circulation depends on identifying lost circulation zones before drilling through geologic analysis of image logs and cores. Geologic and seismic characterization of faults may prove helpful in designing well trajectories that avoid potential thief zones. If the thief zones cannot be avoided, preparing the mud with lost circulation prevention materials, termed Wellbore Strengthening materials, can prove beneficial. Wellbore strengthening involves either continuous mud circulation of particles in the drilling mud or squeezing pills into the formation.

Hesitation squeeze is a squeeze cementing technique where the cement slurry is pumped into the well and waited on in different stages. The pumped cement is exposed to differential pressure higher than the pore pressure in the zone of interest. This differential pressure allows the cement to seep into the fracture until no further cement slurry can be placed. The cement in the zone of interest forms a hydraulic seal with high compressive strength. Formations with low permeability are usually targeted for hesitation squeeze (Dupriest, 2005; Al-Houti et al., 2017).

Particulate materials used in continuous mud circulation are termed wellbore strengthening materials (WSMs). WSMs include calcium carbonates, graphite, sawdust, and graphite. WSMs seal the fracture near the tip, isolating it from the fracture network and wellbore surface. Wellbore strengthening works by increasing the fracture gradient and fracture propagation resistance. Wellbore strengthening has proved successful in high-permeability rocks with natural and induced fractures (Oort & Razavi, 2014).

2.3.2 Remedial Approach

In cases where lost circulation is not anticipated, curing the mud losses is achieved by creating a seal that reduces the effective permeability of the thief zone. This seal reduces the drilling mud losses so the zone can be drilled ahead. It is crucial to determine the location of the thief zone before placing the curing treatment. Mud losses occur at the shoe of the last casing string or higher up the wellbore, not at the drilling bit as previously conceived. Factors influencing the success of lost circulation remedial treatment include fracture size and orientation, effective permeability, and pore size of the thief zone (Messenger, 1981; Alsaba et al., 2014).

Lost circulation treatments can be grouped into the following subsystems:

- lost circulation materials include nut shells, calcium carbonate, walnut, and fibers.
- settable systems.
- blends of settable materials and LCMs.

Lost circulation materials (LCMs) bridge and seal fractures for a certain fracture width. Usually, certain LCMs are effective in specific fracture aperture ranges. LCM particles can only then enter voids or fractures. The LCM particles should be small enough to pass through the fracture opening and large enough to bridge the fracture. The seal becomes ineffective if the LCM

particles seal just the fracture opening without bridging the fracture. The ineffective seal becomes unstable and can be easily destroyed when drilling continues. Granular materials such as particulates, fibers, and walnut have successfully been used in geothermal wells to cure or minimize lost circulation.

In a study by Ezeakacha and Salehi (2018), the authors investigated and quantified the impacts of temperature change, LCM type, concentration, and particle size on dynamic fluid invasion in porous media. Fluid loss experiments were performed with a dynamic radial system and ceramic filter tubes. The results revealed that temperature change substantially affected fluid loss. Statistical analysis of the experimental results showed no significant change in the fluid loss when two different pore throat diameters were considered. LCM types with a wide range of mud PSD are suitable for limestone formations. Rock porosity and permeability are critical factors in designing a preventive LCM mud (Ezeakacha and Salehi, 2019).

LCMs with multimodal PSD have proven successful in field applications in curing lost circulation. The idea is to design a composite material of particles, fiber, and flakes to achieve a multimodal LCM. This design will help improve the fracture sealing properties as the LCM contains various representative PSD sizes (Figure 2.9). The composite materials should be acid-soluble to ensure minimal formation damage while curing losses in the reservoir section (Obando and Fornasier, 2017). The multimodal LCMs successfully sealed a wide range of fractures when tested using a permeability plugging apparatus.

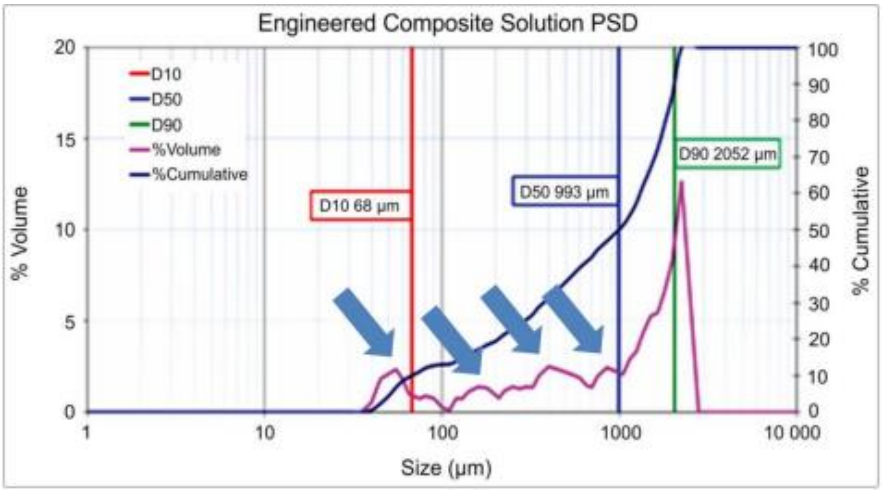

Figure 2.9: Representative size peaks on the multimodal PSD LCM (Obando and Fornasier, 2017)

Although some LCMs were thought to be chemically inert, Vivas and Salehi (2021) showed that some LCMs can affect the rheological properties of the drilling fluid based on the particle size distribution. The authors categorized multiple LCMs into coarse granular, flaky, fibrous, and fine granular. Fibrous materials like sawdust and magma fiber showed a variation of 336% and 283% compared to the base drilling mud with no LCM (Figure 2.10a). In contrast, fine granular materials, including calcium carbonate ($CaCO_3$) and graphite, showed only a deviation of 17.6% from the base mud (Figure 2.10b). The authors concluded that fine granular materials had minimal effects on the fluid rheology compared to coarse granular, flaky, and fibrous LCMs.

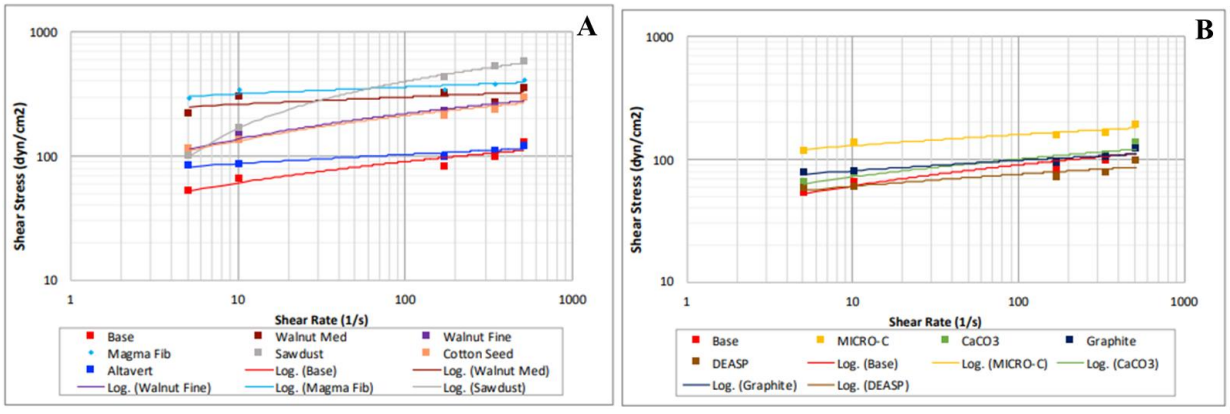

Figure 2.10: Shear stress vs. shear rate of (a) coarsely granular, flaky, and fibrous materials and (b) fine granular materials (Vivas and Salehi, 2021).

Rickard et al. (2010) successfully applied micronized cellulose to minimize lost circulation in the PUNA geothermal wells. The PUNA geothermal well is located on the Big Island of Hawaii, with bottom-hole temperatures reaching 600°F at depths of 5000 ft. The authors reported that micronized cellulose was introduced in the unweighted mud system when lost circulation occurred during drilling. The LCM particles effectively reduced the severity of the lost circulation from critical to minor seepage. When drilling through the pay zone, a high-temperature copolymer drilling fluid conditioned with micronized cellulose was used to protect the reservoir and minimize losses.

Settable systems such as crosslinked gel systems and cement slurries work by developing a solid seal when introduced in the thief zone. The slurries and gel are pumpable and contain little to no solid particles. Settable slurries, unlike particulate LCMs, can enter fractures and voids of any width or aperture. This seal formed is often insoluble and prevents the use of settable systems in pay zones. Additionally, premature gelation can also reduce their sealing capability. Crosslinked gel systems have proved effective in curing lost circulation in vuggy formations.

Al-Azmi et al. (2014) successfully applied a crosslinking polymer fluid treatment to cure severe lost circulation in a fracture limestone formation. The authors showed how careful customization of the setting time of the polymer fluid allowed the polymer fluid to be pumped downhole through the bottom hole assembly, saving rig time and cost. This approach is impossible for conventional LCM, where the drilling string must be tripped out before setting the LCM in the thief zone. Wu et al. (2021) also showed a successful field application of polymer gel in a fractured tight sandstone reservoir.

Based on the field applications listed above, LCMs and settable systems design and optimization are crucial to a successful LCM treatment. Factors such as fracture characterization, fracture width,

LCMs, and polymer concentration must be considered. The system should be designed to be easily pumpable through the downhole equipment, compatible with the well fluids, strong enough to withstand wellbore pressure, and nonhazardous to the pay zone (Doger et al., 2014; Alsaba et al., 2014). Table 2.1 lists examples of LCMs and porous media used for testing.

Table 2.1: Examples of polymer-based LCMs and porous media

Type of LCM	Porous Media	Outcome	Reference
Polyacrylamide/phenol-formaldehyde (PAM/PF) gel	see-through flow pack with varying permeability	Prevent fluid losses in 2/3 of the porous media	Hashmat et al., 2017
Oil Absorbent Polymer (OAP)	Tapered metal slots with sizes 0.2, 0.5, and 1.0 mm	Poor fracture sealing capacity but decreased fluid loss when blended with other materials	Zhong et al., 2018
Polyacrylamide/Polyethyleneimine (PAM/PEI) gel	Ceramic discs	Reduced fluid loss by up to 80% compared to base mud	Magzoub et al., 2020
Polyacrylamide/Polyethyleneimine (PAM/PEI) gel	Aluminum discs	Cumulative fluid floss only 30 cc, with sealing pressure up to 2000 psi	Magzoub et al., 2021
Polyacrylamide/triamine functionalized silica (PAM/FNS) gel	API fracture discs	Filtrate volume reduced to 25%, and sealing pressure up to 1000 psi	Magzoub et al., 2021
Blend of SMP and fiber	fractured granite cores	6 wt% SMP was capable of sealing large fractures sizes of 3000 μm	Magzoub et al., 2021
Smart anionic shape memory polymer activated by heat (70°C)	API fracture discs	The proposed smart anionic SMP showed capabilities of sealing fractures sizes ranging from 1.25 - 2.5 mm	Mansour and Taleghani, 2018
Smart LCMs	Slotted discs	Minimized fluid loss and induced compressive stress to strengthen the wellbore	Mansour et al., 2017
Multiple particulate LCMs, including fiber, micronized cellulose, graphite blend	API fracture discs	Found granular blended materials performed better than fibrous materials	Vivas et al., 2022
SMP	3D fractured disc in a large flow loop	SMP suspended in a large flow loop and sealed fractured disc	Mohamed et al., 2022
Shape memory polymer (SMP)	Additive fractured disc and metal fracture disc	The cumulate fluid loss was reduced by 71%, and sealing pressure increased by 60% when comparing additive fracture disc to metal disc	Vivas et al., 2022b

2.4 Shape Memory Polymers

Shape memory polymers (SMP) are particulate LCMs that can be transformed into a temporary shape under external stimuli such as heat, light, moisture, magnetic field, or pH. Other polymers like rubber can change their shape when loaded with some external stimuli but return to their normal state when the stimuli are removed. However, SMP becomes deformed when loaded with external stimuli and can trap the mechanical energy applied. Unlike other polymers, shape memory polymers possess these shape-changing advantages and are inexpensive, lightweight, nontoxic, and biodegradable (Li, 2004; Ratna & Karger-Kocsis, 2008).

Shape memory polymers (SMP) are considered polymeric smart materials. SMP is made by heating the polymer to a particular temperature known as the programming temperature. An external load is applied to deform the SMP to a temporary shape during heating. Then, the polymer is cooled below its glass transition temperature (Mohamed et al., 2021). The glass transition temperature is the temperature below which an amorphous materials transition from viscous and rubbery into hard and glassy. (Dyre, 2006) Once the load is removed, the SMP is expected to maintain this deformed shape, as shown in Figure 2.11a. When the SMP is heated to a temperature higher than the programmed temperature, the stored mechanical energy will be released and the original shape restored, as shown in Figure 2.11b (Liu et al., 2009).

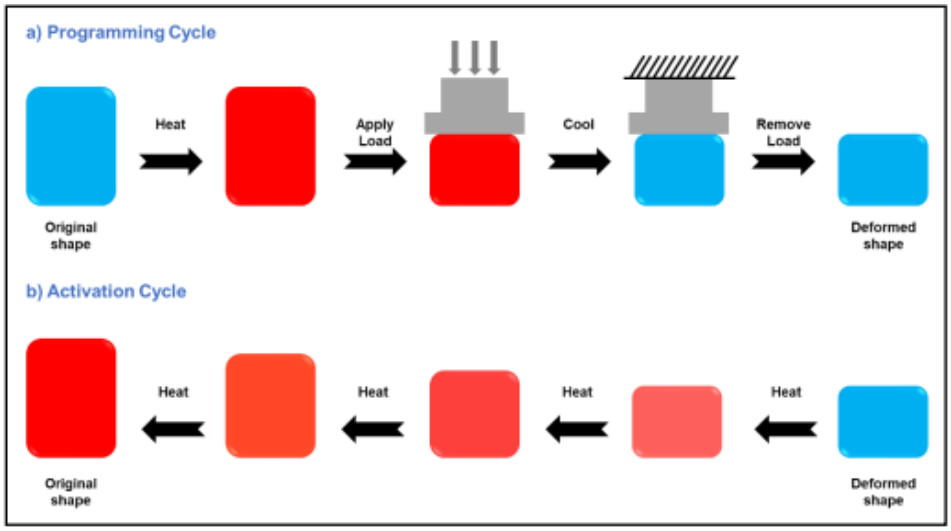

Figure 2.11: Programming and activation of shape memory polymers (Mohamed et al., 2021)

Thermally-induced SMP responds to temperature as the primary external stimulus. They are the most common SMP, and the transformation of the physical properties occurs at the critical temperature. The shape memory materials are then fixed into a temporary shape and can later regain their original shape by heating above their transition temperature. The transition temperature is the glass temperature for amorphous thermoset SMPs (Magzoub et al., 2020; Mansour et al., 2017). SMPs have been known to recover strains of up to 800%. (Voit et al., 2010). Figure 2.12 shows the deformation and recovery process.

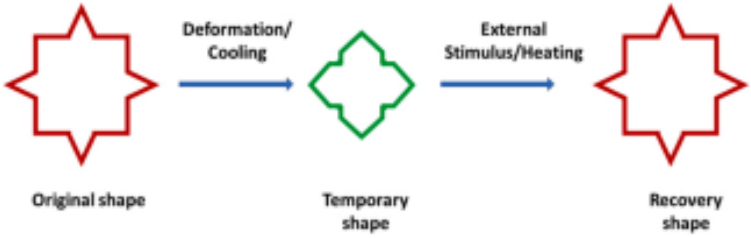

Figure 2.12: Deformation and shape recovery for thermosets SMP (Magzoub et al., 2021)

The shape memory polymers have an active phase and a frozen phase. The active phase is exposed to softening and hardening upon removing and applying the external stimuli. The frozen phase remains hard during the shape-changing process. For a thermoset SMP, the softening of the

SMP acts as a medium to store mechanical energy during programming either by increasing enthalpy, decreasing entropy, or both. The hardening of the SMP is formed by crosslinking, which restricts neighboring chains from slipping during deformation and consequent build-up (Srivastava et al., 2017).

Polymers can be crystalline or amorphous, and the crosslinking type can be chemical, physical, or composite. The shape memory effect of the SMP is not linked to specific material properties but rather the polymer structure and morphology combination in addition to the programming technology (Li et al., 1998). The programming of the SMP involves repeated deforming and shape recovery under external stimuli to yield a stress-strain curve. (Li and Xu, 2011).

Previous studies on SMP showed that they could be activated at specific temperatures, making SMP useful for loss circulation prevention in high-temperature environments and geothermal drilling. Mansour et al. (2017) applied a smart LCM in sealing fractures and lost zones. This smart LCM is based on a shape memory polymer thermally activated by the formation's natural heat. The activated LCMS expands and can seal fractures' width without damaging the productive zones or drilling tools. The activated temperature of the proposed smart LCM by the authors was based on the reservoir formation (70°C) and is adjustable. Further volumetric strain testing revealed the smart LCMs were expandable, but there was no change in mass. This finding corroborated the assumption that the smart LCMs will recover their original shape under high pressure.

Another study by Magzoub et al. (2021) was performed on a blend of fiber and shape memory polymer (SMP) at temperatures up to 150°C. To simulate conditions in geothermal formations, the author tested the blend on a granite core using a novel flow loop to simulate fracture

loss at dynamic conditions. Their analysis showed that an LCM blend of 6 wt% SMP and 5 lb/bbl fiber could seal a 3000 μm fracture with sealing pressure up to 500 psi. Generally, the authors confirmed that blends of SMP and fiber performed excellently than either SMP or fiber, as presented in the findings of Mansour et al.

Mohamed et al. (2022) conducted experiments on a large-scale flow loop to investigate SMP's rheological performance and annular flow. The SMP's rheology, wellbore hydraulics, settling behavior, and activation process are studied under different dynamic conditions. The authors found the shape of the SMP increased by 80-100% of its original size. No additional frictional pressure losses were observed when the SMP was added to the base drilling fluid. Successful suspension of the SMP at 1 wt% was observed; increasing the concentration to 3 wt% led to settling and forming a bed on the drill pipe. All these factors are important considerations for the optimization of SMP.

This study evaluates SMP's sealing and bridging efficiency to plug complex fractures as observed in geothermal formations. The rheology, particle size distribution, and seal capabilities are observed and discussed. The experiments were conducted at high temperatures of up to 200°F, and the complex fracture was designed using a 3D-printed disc. This study aims to investigate the performance of SMP as a suitable particulate LCM candidate in high-temperature wells.

2.5 Settable Systems Based on Crosslinked Polymers

2.5.1 Theory and Chemistry of Crosslinking

Crosslinking is the process of linking together polymer chains, and it is usually accomplished by introducing a crosslinker between polymer chains. In a typical crosslinking reaction, a small molecule, called a crosslinker, is introduced to a base polymer solution. Crosslinkers can be either

bi- or multi-functional, depending on their number of reactive groups. Crosslinkers with more than two reactive groups can simultaneously react with multiple polymer chains (Mizsei et al., 2021).

Crosslinked polymers are usually synthesized in solution, where the crosslinker and polymer are dissolved in a solvent. The resulting solution is then mixed and heated to a high temperature for the crosslinker to react with the polymer. Crosslinked polymers can also be synthesized in the melt, where the polymer is heated to a high temperature for the crosslinker to react with the polymer (Reyes-Labarta et al., 2011).

Base polymers such as polyacrylamides (PAM) and polyacrylamide tert-butyl acrylate (PAtBA) are often crosslinked with organic and inorganic crosslinkers. PAM is a high-water absorbent polymer that forms a soft gel when hydrated in a solvent (Shamlooh et al., 2019). As depicted in Figure 2.13, the amide group in the structure of PAM is made up of a carbonyl functional group with the carbon atom double bonded to an oxygen atom (C=O), one nitrogen and two hydrogen atoms (CONH2) (Uranta et al., 2018). Similarly, the PAtBA structure showed the methyl carbon attached to the tertbutyl acrylate groups (CH3)CONH2, the methine carbons attached to the amide groups (CH)COO, and the methine carbons to the carboxylate groups (CH)COO ((Halverson et al., 1985; Moradi-Araghi et al., 1988).

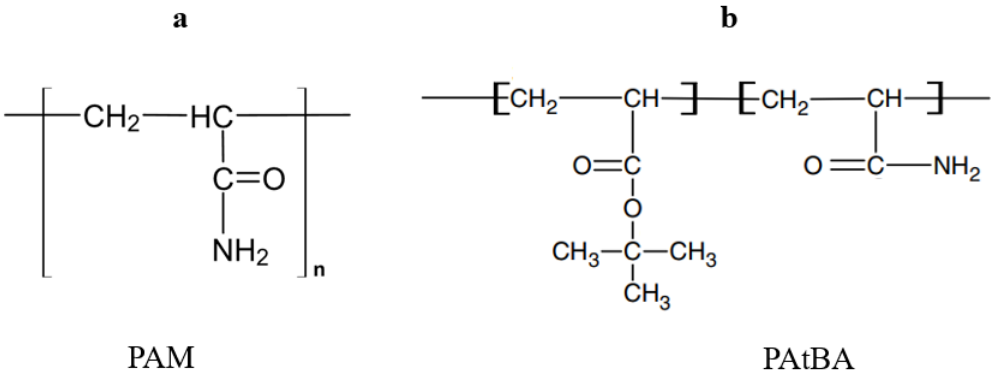

Figure 2.13: (a) Chemical structure of Polyacrylamide (PAM): n denotes the number of repeating units and (b) polyacrylamide tert-butyl acrylate (PAtBA) (Al-Muntasheri et al., 2008)

It is believed that nucleophilic substitution processes of the tBA component play a significant role in the crosslinking of PAtBA with PEI. Crosslinking PAtBA with PEI forms a thermally stable covalent bond because of the carbonyl carbon and amine nitrogen reaction, as described in Figure 2.14. The PEI reaction does not require hydrolysis (or thermolysis) of the crosslinking site, thus, helping PEI to propagate efficiently through the rock under reservoir conditions. On the other hand, the crosslinking reaction between PEI and PAM is thought to occur between the imine nitrogen on PEI and the amide groups on the PAM (transamidation), as shown in Figure 2.15.

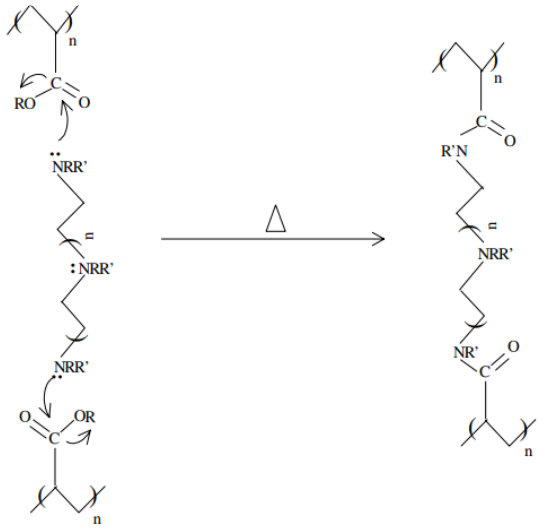

Figure 2.14: Crosslinking of PAtBA with PEI (Hardy, 1999)

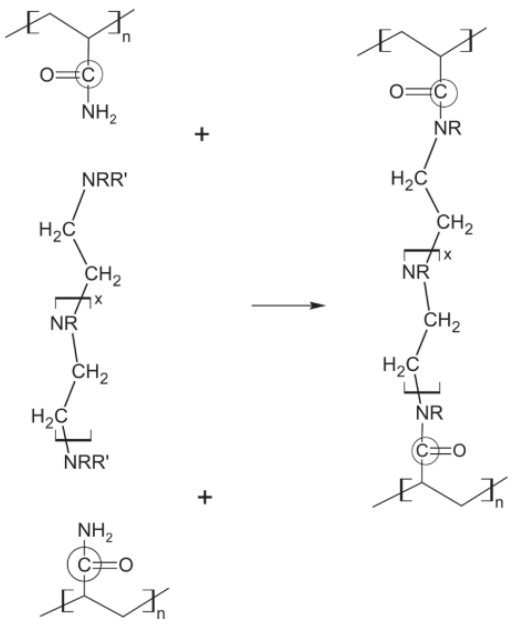

Figure 2.15: Crosslinking of PAM with PEI (Reddy et al., 2003; Al-Muntasheri et al., 2006)

The key difference between different base polymers is thermal stability, molecular weight, and degree of hydrolysis. Copolymers of acrylamide and t-butyl acrylate (PAtBA) have been used as base polymers crosslinked with PEI. This base polymer is prepared with as few acrylates for crosslinking control. A low degree of hydrolysis (<1%) usually translates to a low crosslinking rate. (Bryant et al., 1997). This low degree of hydrolysis, in turn, helped enhance the thermal stability of the final gelled material.

Crosslinking rates for these polymer systems are usually controlled by varying the crosslinker concentration, solution pH, polymer hydrolysis, adding accelerators (ligand) and retarders (chelator), or any combination of these. The chemical properties of the base polyacrylamide polymer usually control the crosslinking rate. Essentially, the crosslinking rate is lowered by adding chemicals to the polymer gel that are initially inert and become more reactive after extended exposure to reservoir conditions (Hardy et al., 1999).

Magzoub et al. (2021) investigated the viscosity of three polymers with low, medium, and high molecular weights to show how the molecular weight affects the crosslinking rate. The high molecular weight PAM (>1.5x105 Da) showed a higher viscosity magnitude, more than three times when compared to the low and medium molecular weight PAM, as shown in Figure 2.16. The gelation occurred for all samples at about 90 minutes. The rate of gelation and viscosity was shown to be highly dependent on the molecular weight of the PAM.

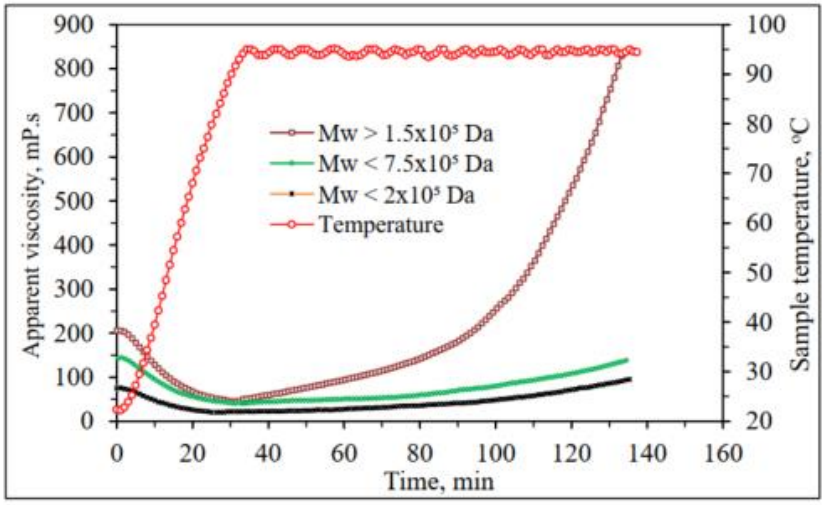

Figure 2.16: Impact of PAM molecular weight on gelation kinetics in salt-free water (Magzoub, 2021)

2.5.2 Gelation kinetics

The gelation time is the time required for a crosslinked polymer to begin thickening under certain conditions, termed crosslinking induction period (Prud'homme et al., 1983). The effects of temperature, pH, salinity, clay particles, pipe rotation and shearing, stress, and oilfield contaminants on crosslinking induction are defined so that there is sufficient time for the crosslinked polymer formulation to be placed in the target location downhole.

The inflection point on the viscosity vs. time curve for the crosslinked polymer formulation closely corresponds to the time the fluid viscosities begin to increase. This idea leads to plotting the viscosity vs. time curves of crosslinked polymer samples heated to a particular temperature to

determine the gelation time, as shown in Figure 2.17. The results showed the gel time for a crosslinked PAtBA with PEI to be 1.6 hours (Hardy et al., 1999). To ensure accuracy and consistency, the authors used two different viscometers, Brookfield RVT II+ and Fann Model 50.

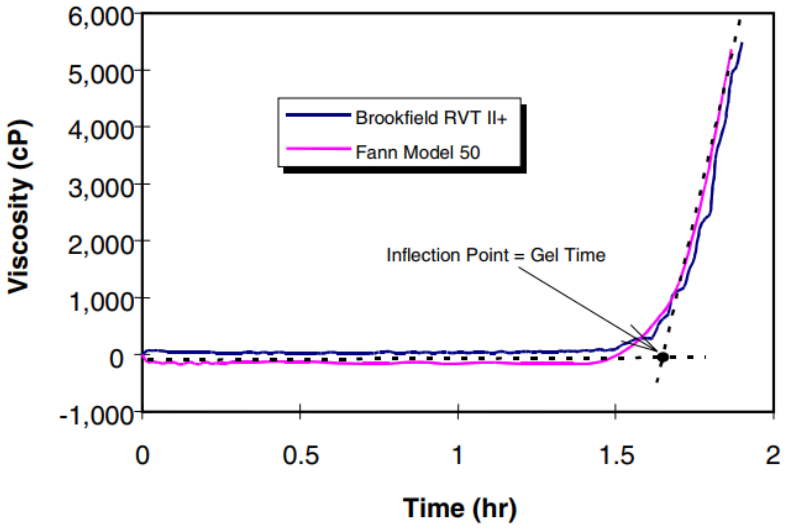

Figure 2.17: Comparison of Gel Times of Identical Organically Crosslinked Polymer Formulations Obtained at 96° C using Different Viscometers (Hardy et al., 1999)

Furthermore, the effect of crosslinker concentration is an essential aspect of gelation kinetics. In literature, the crosslinker concentration has been found to have a more significant effect on gel strength than the viscosity of the polymer system. For a PAM/PEI system, the authors found that increasing the PEI concentration from 0.25 wt% to 1 wt% showed little to no effect on the apparent viscosity of the system, as described in Figure 2.18. However, there is a significant increase in the 30 mins gel strength from 0.5 wt% PEI to 0.75 wt% (Magzoub et al., 2021).

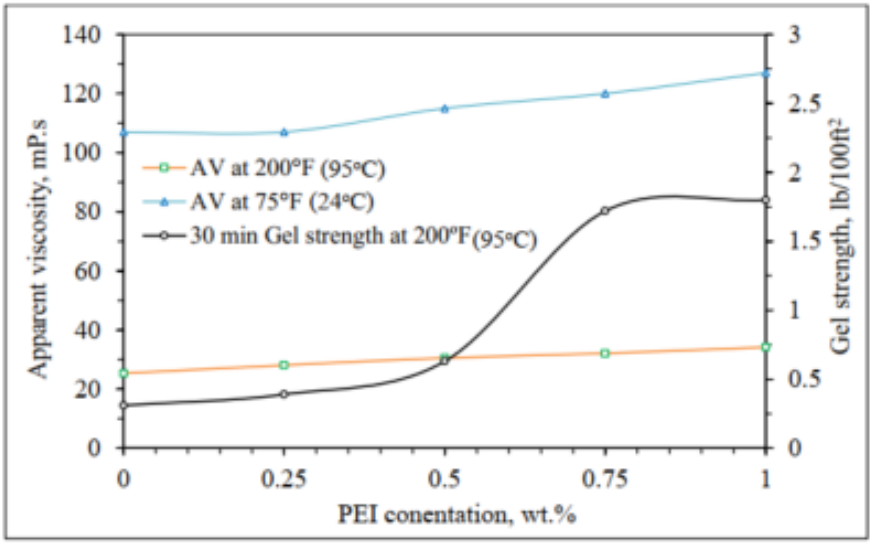

Figure 2.18: Effect of PEI concentration on AV, PV, and Gel Strength (Magzoub, 2021).

Controlling parameters that significantly affect the gelation kinetics and time include polymer concentration, crosslinker concentration, the ratio of the retarder to crosslinker, pH of the crosslinker, temperature, and salt concentration. Jayakumar and Lane (2012) summarize the investigation results of the parameters in Table 2.1. A decrease in the concentration of the polymer and crosslinker lead to an increase in the gelation time. On the other hand, an increase in the DS: PEI ratio, crosslinker pH, and salt concentration led to an increase in gelation time. Increasing the temperature accelerated the gelation process, thus decreasing the gelation time.

Table 2.2: Effect of various parameters on gelation time (Jayakumar & Lane, 2012)

Parameter	**When the parameter**	**Gelation time**
Polymer concentration	Decreases	Increases
PEI concentration	Decreases	Increases
The ratio of DS: PEI	Increases	Increases
pH of PEI	Increases	Increases slightly*
Temperature	Increases	Decreases
Salt concentration	Increases	Increases

*(pH range: 9 – 10.65)

2.5.3 Crosslinked Polymer Systems as Lost Circulation Materials

This section reviews the application of crosslinked polymer systems in plugging lost circulation zones in the oil and gas industry. Using crosslinked polymer systems to plug lost circulation zones has begun to take shape in the oil and gas industry. The idea is to mix the polymer with the drilling mud and then pump the polymer mud downhole as a single solution or separate pill to act as a sealing barrier for the fracture (Hamza et al., 2019).

In practice, the crosslinked system is activated by temperature, time, or the shearing of the drill string and bit. After the polymer has been set at the thief zone, the pill produces a rubbery, slippery substance that seeps into the fracture and voids and prevents additional mud losses. The time it takes the pill to transition from liquid to its rubbery solid-like state is the setting time and can take minutes or hours. Retarders can be used to increase the setting time, while accelerators are used to decrease the setting time. The decision to use a retarder or an accelerator depends on the depth of the thief zone and bottom-hole temperature (Wang et al., 2008; Caughron et al., 2002).

Polymers of polyacrylamide tert-butyl acrylate (PAtBA) have been crosslinked with polyethyleneimine (PEI) for water shut-off gel operations and conformance control applications (El-Karsani et al., 2015; Shamlooh et al., 2020). Polyacrylamide (PAM) has recently been used over PAtBA for economic and environmental reasons (El-Karsani et al., 2013). PAM/PEI gels have been shown to have faster gelation time, lower activation energy, more stability, and more crosslinking than PAtBA/PEI gels (Al-Muntasheri et al., 2006; El-Karsani et al., 2013; M. I. Magzoub et al., 2021).

A crosslinked polyacrylamide LCM was developed and applied successfully to mitigate lost circulation in multiple wells in the Gulf of Mexico at low temperatures (Bruton et al., 2001; Ghriga et al., 2019; Sweatman et al., 2007). Magzoub (2021) investigated the use of multiple

chemical agents, including Aluminum acetate (AlAc), triamine functionalized silica (FNS), and polyethyleneimine (PEI) in crosslinking with low molecular weight PAM. All three crosslinked polymers showed comparable results in the sealing experiments, with the PAM/FNS polymer gel having the least filtrate loss and highest sealing pressure.

The use of polymer LCMs has been limited to low-temperature reservoirs. In high-temperature and high-pressure (HPHT) formations, reports of leakage have been known to occur due to different lithology types in the rock strata (Mirabbasi et al., 2022). The rheology and stability of polymer mud are essential parameters; therefore, experimental work is needed to investigate the performance of PAM/PEI gels to prevent the lost circulation at high temperatures up to 150°C (302°F). Using polymeric gels as LCM can help minimize the risk of formation damage caused by drilling filtrates. The filtrates are usually formed near the wellbore due to overbalanced drilling. As the crosslinked polymer activates at high temperatures, a mature gel is formed with a dense uniform structure that can withstand up to 1000 psi (Magzoub et al., 2021).

This study investigates the effects of various parameters on the efficacy of the PAM/PEI gel systems as lost circulation plugging gels using acid rheometers and permeability plugging tests at high temperatures. The parameters include the effect of varying concentrations of crosslinker and polymer, pH, gelation time, and plugging efficiency. Most previous works did not consider the gel's dynamic evolution, achieved using the acid rheometer. In addition, we investigated the ability of the gels to plug tapered fractures up to 1 inch long. This improved methodology will be beneficial in selecting the appropriate concentrations of polymer and crosslinking agents in plugging fractures in high-temperature oil, gas, and geothermal reservoirs.

2.6 Lost Circulation Materials Testing

Laboratory testing of proposed lost circulation materials (LCM) is vital for successful lost circulation treatment. The LCM quality is usually based on the total fluid loss within a specified time and the maximum differential pressure it can withstand before failure. These parameters are usually evaluated by filtration into a porous media, metal, or ceramic disc. Multiple researchers have tried to quantify the sealing properties of multiple LCMs. For example, Magzoub et al. (2021) used a new type of engineered LCMs -Shape Memory Polymers (SMP)- and fiber additive in sealing possible fractures encountered during geothermal drilling. They described the effect of fracture opening size on the LCMs.

Vivas and Salehi (2021) tested multiple LCM, including cottonseed hulls, calcium carbonate (CaCO3) blend, walnut fine and medium, sawdust, graphite blend, and micro cellulose (Micro-C) at elevated temperatures for geothermal applications. They tested these materials at 302°F using a high-temperature, high-pressure (HPHT) filtration cell. They showed that some materials were sensitive to high temperatures and degraded under heat, while others were thermally stable (graphite, CaCO3, and Micro-C). They also showed the importance of particle size distribution (PSD) in evaluating the efficiency of LCM in sealing and bridging fractures.

Khalifeh et al. (2019) developed two LCMs (M and C) with dynamic differential pressures exceeding 2000 psi to understand the effect of fracture opening size and differential pressure. The fracture size ranged from 400 to 2500 μm. Next, drilling mud was pumped through the test cell, forming a filter cake across the disk slot. The maximum pressure required to break the seal is obtained except in cases where the pressure exceeds 5000 psi due to system limitations. The results shoed that fluid loss strongly depends on the LCM concentration and is summarised in Figure 2. 19.

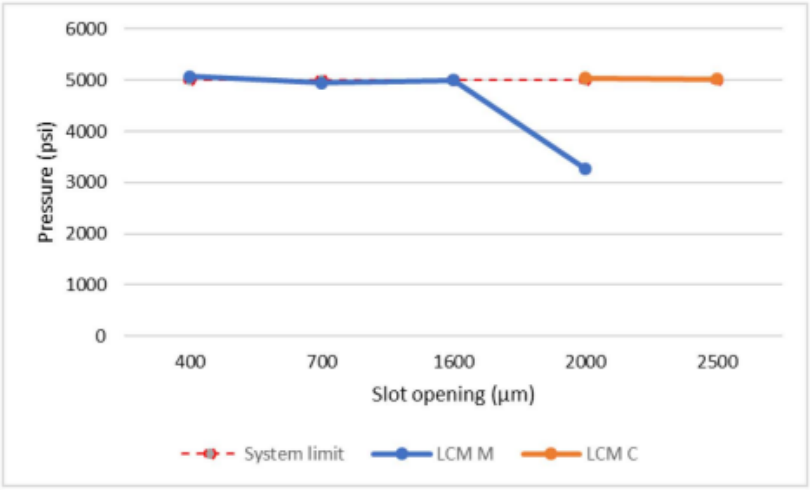

Figure 2.19: Summary of test results for sealing slots

Hitchcock (2021) showed the ability to plug larger fractures ranging from 4mm to 20mm by extending the plugging range of conventional LCMs with an additively manufactured shape. The supplement additive manufactured shape was designed as a hollow perforated shape and tested on more extensive fractures associated with total lost circulation events. The experiment was conducted on a custom apparatus with two fluid circuits and a test orifice using a simple test fluid.

2.6.1 Fracture type for testing LCMs

Understanding the formation of fractures involves knowledge of geology and geomechanics of the formation, fracture type, internal structure, and network patterns. The geometry, fracture architecture, and stress system affect how fluid moves through fractured rocks. Stress heterogeneity and concentration control the initiation and propagation of discrete fractures and the localization and clustering of fracture systems. Rock properties are also crucial to the formation and structure of fracture systems (Park, 2005).

Commonly occurring fractures can be divided into (1) extensional fractures and (2) shearing fractures, depending on the type of displacement discontinuity (Figure 2.20). Extensional fractures exhibit extension perpendicular to the walls of the rock surface. Even though most joints

have only a slight extensional displacement across the joint surfaces, they are nonetheless considered real extension fractures because there is little to no macroscopically apparent displacement in the joints. A fracture along which the relative movement is parallel to the fracture is known as a shear fracture or slip surface. Shear fractures are defined as fractures with modest displacements (mm to dm scale), whereas faults are more frequently defined as discontinuities with bigger offsets (Van Der Plujim and Marshak, 2004; Petrov, 2013).

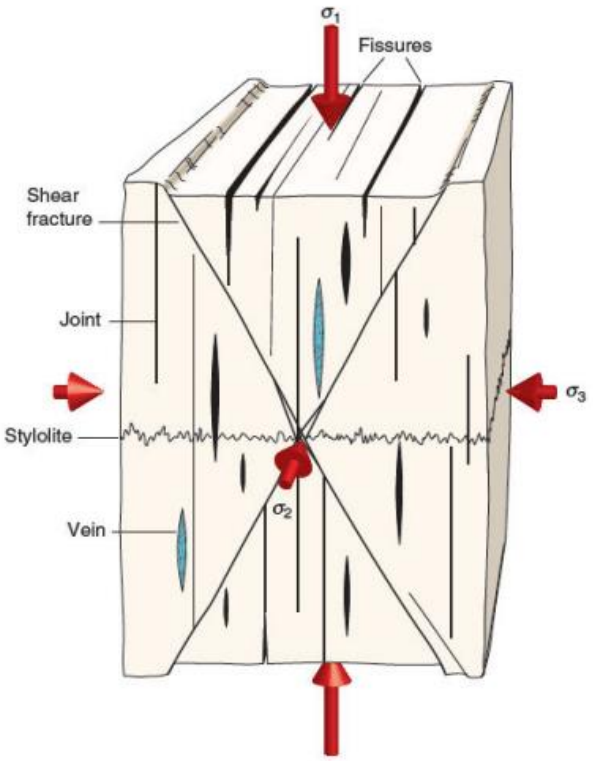

Figure 2.20: Orientation of various fracture types with respect to principal stresses

2.7 Application of 3D printing for Testing LCMs

Additive Manufacturing, or 3D printing, refers to the technology that uses various manufacturing methods by adding materials layer by layer. In contrast, Subtractive Manufacturing involves materials being removed from a built part. The intention is to make products through processes such as milling or turning (Ford & Despeisse, 2016). Additive Manufacturing has recently been

used in multiple industries, from biomedical to automotive. Additive Manufacturing has allowed rapid prototyping of tools leading to direct production. Its integration with computer numerical control (CNC), computer-aided design (CAD), and manufacturing is crucial. Materials mainly used in these industries include metals, polymers, ceramics, and composites (Cooper, 2001; Zhong et al., 2017).

Additive Manufacturing has recently gained momentum as an alternative process in the energy, marine, oil, and gas industries. This manufacturing method offers significant advantages to these industries. A flexible supply chain and new optimized and simplified designs make the path from design to production faster and more comfortable (Imrie, 2017). Additive manufacturing can also increase the available technology in the geothermal industry by reducing costs associated with fabricating complex components and low-volume parts, especially where specialized tools are required (Polsky et al., 2020).

Some researchers have studied the application of 3D printing in the oil and gas industry. For example, Jiang et al. (2016) examined the use of 3D printing on the dynamic fracturing of rocks. They experimented with gypsum-like powder material in printed rock specimens and produced specimens for the dynamic Split Hopkinson Pressure Bar (SPHB) test. They concluded that adequate sample preparation for 3D printing would make it highly competitive. In addition, stated quickness to prototyping, geometry flexibility, and material homogeneity give a competitive advantage of 3D printed rocks over other processes. Finally, they demonstrated that the 3D-printed rock specimen mimicked traditional brittle rock-like materials in rock dynamics testing.

Zhou and Zhu (2017) investigated the tensile fracture behavior of both natural and artificial rock materials. The authors investigated ceramic, resin (accura® 60), acrylic copolymer (SR20), polymethyl methacrylate (PMMA), and gypsum. Uniaxial compression tests were performed on

five artificial rock samples. The results showed that the resin sample simulates the most hardened and brittle rock material. They finally tested a resin specimen to mimic a natural rock sample by performing a static and dynamic Brazilian disc test.

Yang et al. (2020) utilized 3D printing to improve the applications of the micro model of a sample rock. They accounted for numerous factors, including pore-filling multi-scale, wettability, and surface tension. They demonstrated the ability to replicate carbonate rocks' complex fracture-vug structure and flow characteristics. 3D models were built considering crucial parameters such as geometric features and the similarity of dynamics. Finally, experimental tests on the 3D-printed samples were used to investigate multiphase flow behaviors on rocks.

This study explores the use of 3D printed materials in testing for lost circulation materials (LCM). Because of the hostile and heated conditions of the geothermal environment, not all 3D printing materials can withstand the expected elevated temperatures (usually greater than 150F). Nylon Carbon Fiber (nylon C.F.) is the most suitable for this use. Other materials such as polylactic acid (PLA), Polyethylene, Terephthalate Glycol (PETG), and Acrylonitrile Butadiene Styrene (ABS) were considered but deemed unsuitable for geothermal applications because of their lower temperature deflection. This study also investigated the sealing efficiency of Shape Memory Polymers (SMP). We used 3D-printed nylon C.F. discs in a permeability plugging testing apparatus. A more realistic fracture orientation with multiple fracture sizes and tapered length were designed and investigated.

Chapter 3 : Laboratory Experimental Methods

This chapter describes the experiments conducted for testing lost circulation material (LCM) using 3D-printed fractured discs. The design of experiments, testing procedures, materials, and experimental methods are presented in this section.

3.1 Design of Experiments

Different concentrations of shape memory polymer (SMP) in water-based mud solution were evaluated for use as LCM in bridging and plugging fracture openings. Then, the capabilities of SMP were compared with the widely used industry LCM, walnut.

Finally, we investigated the optimization of multiple combinations of polymers and crosslinkers for potential use as LCM in plugging tapered fractures. The polymer gel system comprises polyacrylamide as the base polymer and polyethyleneimine as an organic crosslinker. Figure 3.1 shows the workflow set up to realize the objectives of this study.

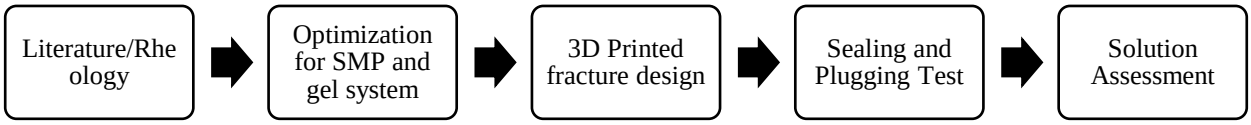

Figure 3.1: Workflow Design employed in this study

3.2 Materials

This section discusses the materials used in this study, including shape memory polymers, polymeric mud solutions, and walnut. Also, the 3D printing materials and the process is presented.

3.2.1 Shape Memory Polymers (SMP)

One LCM used in this experiment is a shape memory polymer (SMP). The SMP is a granular type of LCM, as shown in Figure 3.2b. SMPs are polymers that can be deformed to a temporary shape. The temporary shape can recover its original shape under external stimuli such as temperature,

light, or moisture. The SMP used in this study is a thermally activated polymer. The SMP was synthesized from a commercial epoxy resin (EPON 826) and cured by an IPD (isophorone diamine) crosslinker. After mixing and separating air bubbles from the mixture, the polymer was cured at a temperature of 302°F. A thermoset network is achieved after curing, and the SMP is programmed by uniaxial compression. Afterward, the SMP is crushed into smaller-sized grains with particle sizes ranging from 0.6 to 2.14 mm. Magzoub et al. (2021) investigated the particle size analysis (PSD) of this SMP. They found the SMP to have larger particles than fibers with a D50 of 1637 microns. Fan & Li (2018) characterized the thermo-mechanical properties of this high enthalpy storage thermoset SMP. This study investigated the effects of the LCM concentration in bridging and sealing the 3D-printed disc. The weight concentration varied between 1% and 5%.

3.2.2 Crosslinked Polymer Solution

Another LCM considered in this study is PAM/PEI gel mud. When the base polymer, Polyacrylamide (PAM), is crosslinked with Polyethyleneimine (PEI), the gel formed is used in mitigating lost circulation while drilling with water-based mud. With the chemical formula (-CH2CHCONH2-), PAM has a linear chain structure, a low molecular weight of <2 x 105 Da, a specific gravity of 1.036, and is highly hydrophilic. For this study, the commercial PAM obtained has a concentration of 20 wt% in solution, a viscosity of 0.146 Pa.s (146 cp) at 150°C (302°F), and a constant shear rate of 170 s^{-1}. This study investigates using a branched polyethyleneimine (PEI) with the chemical formula (C2H5N)n as the crosslinking polymer. PEI has a molecular weight of 750,000 Da with a concentration of 33.3 wt% in solution. The PAM and PEI were mixed with water-based mud with a density of 8.62 ppg to form the polymer mud.

3.2.3 Walnut

Walnut is a conventional LCM used in the oil and gas industry for decades. They are usually available in fine, medium, and coarse particles. Walnut possesses high compressive strength that makes them effective LCM. Walnuts are used in preventing moderate and severe losses. They provide bridging properties and are efficient when mixed with particulates of other sizes and shapes to provide optimal control. They have also been used historically in reducing the coefficient of friction for drilling muds. For control and benchmarking purposes, the performance of walnut (Figure 3.2a) is evaluated and compared to that of SMP (Figure 3b).

Figure 3.2: Images of (a) walnut and (b) SMP used in this study

3.2.4 3D Printing

The 3D printer in this study utilizes the Fused Deposition Modeling (FDM) technique, which uses a thermoplastic polymer as a filament to create three-dimensional objects. With this printer, the filament is pushed through the hot extruder at 250 °C (482 °F). The filament is first heated and then deposited on a build plate through the heated nozzle layer by layer. The 3D printer uses a uniquely heated and sealed chamber to ensure high dimensional accuracy. Figure 3.3 shows the image of the 3D printer used in this study.

Figure 3.3: Image of 3D Printer (MakerBot Method)

One benefit of using 3D printed discs over conventional metal discs is the ability to create unique fracture designs from wellbore images. This flexibility allows researchers to reproduce designs faster than otherwise with metal discs. (Anyaezu et la., 2021, Vivas et al., 2022).A sketch of the fracture was first drafted from real-time photos of wellbore fractures. This sketch was then transformed into a 3D model designed using Computer-Aided Design (CAD) software. Finally, the 3D modeled fracture is fed to the 3D printer in an STL (Stereolithography) file format. The printing process can take hours, depending on the complexity and slicing properties of the design. This process is described in Figure 3.4.

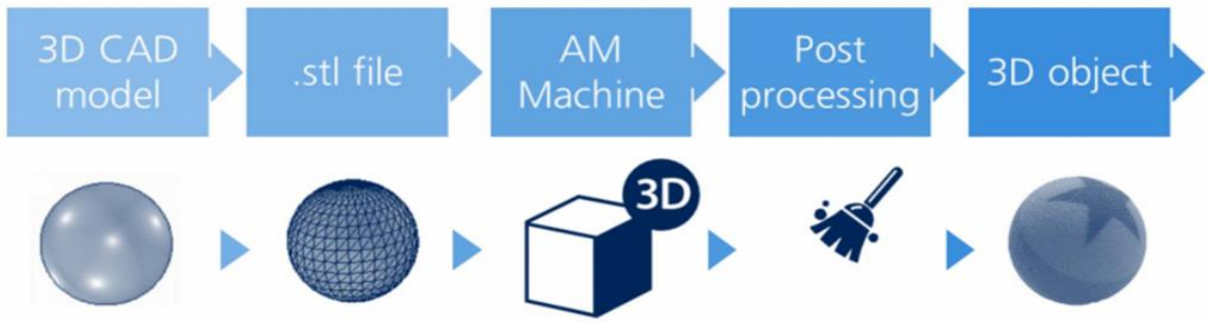

Figure 3.4: The figure above is a typical process path for a 3D-printed component (Imrie, 2017).

3.2.5 Fracture Design

The 3D-printed disc in Figure 3.5 has a diameter of 63.4 mm (2.5 in) and a thickness of 6 mm (0.236 in). For the fracture face, the lateral fracture has a length of 40 mm (1.575 in) and a fracture width of 1500 microns. Each vertical fracture wing has a length of 20 mm (0.787 in) and a fracture width of 1000 microns. Thus, the total surface area of the fracture opening is 100 mm^2. This distinctive complex fracture design provides unique insight into the sealability of the LCM tested.

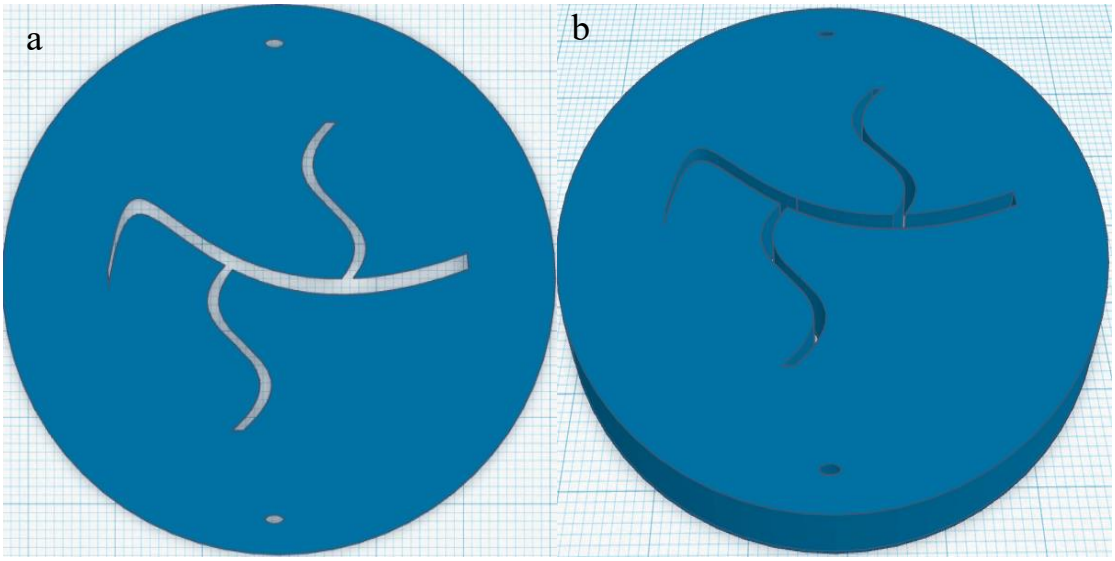

Figure 3.5:(a) 2D and (b) 3D view of the printed disc with complex fracture design.

As for Figure 3.6, the 3D printed disc has a diameter of 63.4 mm (2.5 in) and a thickness of 25.4 mm (1 in). For the fracture face, the lateral fracture has a length of 63.4 mm (2.5 in) and a fracture

width of 38 mm (1.496 in). This tapered fracture design can provide insight into losses in drilling-induced fractures.

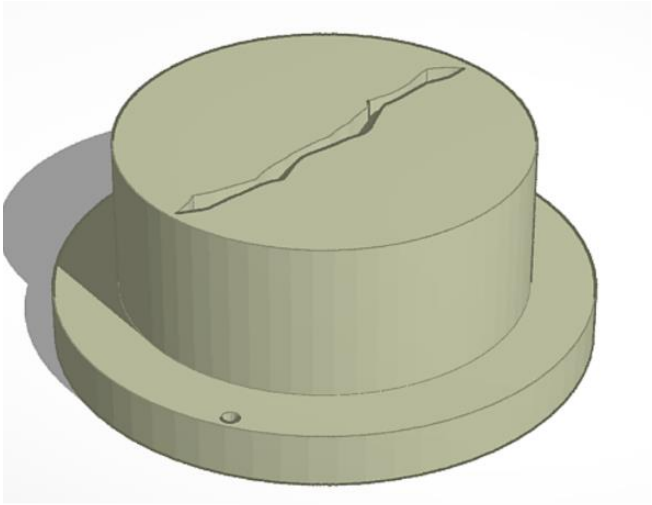

Figure 3.6: 3D view of the printed disc with tapered drilling-induced fracture design.

3.3 Methods

3.3.1 Particle Size Distribution Analysis

The particle size distribution of the particulate LCMs used in the study is measured. The PSD of SMP and walnut are measured with the sieve analysis shown in Figure 3.7. When setting up the sieve analyzer, about 100 g of each LCM sample is placed on the topmost sieve. The sieve analyzer is then operated at a constant frequency for 20 minutes. This motion forces the particle to move down through the different sieve trays.

Figure 3.7: Sieve Analyzer used for determining the PSD for SMP and walnut LCM

3.3.2 Rheology Testing

The first stage of this study includes mud preparation, mud mixing, and rheology testing to investigate the influence of mixing order on the mud properties, gel strength, and onset of mud gelation. While mixing the drilling mud, bentonite was added first before the PAM solution to prevent the flocculation of bentonite. The mixing of the mud additives was done with a standard mud mixer. Rheology tests were conducted using an HPHT Acid Rheometer at a static pressure of 22.3 bar (300 psi), a constant shear rate of 170 s-1, and a rotational speed of 200 rpm while ramping up the temperature to 150°C (302°F). The temperature was then held constant at 150°C (302°F) until the end of the experiments. The viscosity and temperature profile versus time is obtained for multiple PAM and PEI concentrations. PAM varies from 6 to 7 wt% and PEI from 0.5 to 1.25 wt%. Tables 3.1 and 3.2 show the materials and experimental matrix for the rheology study. Results from the multiple rheology profiles are studied and examined, and the optimum concentration is determined. The onset of gelation is observed, and the gelation time is recorded.

Table 3.1: Materials used in the rheology study

Materials	**Property**	**Weight %**	**Volume %**	**lb/bbl**
Water	Base Fluid	70.5%	93.1%	324.6
Bentonite	viscosity control	1%	0.7%	2.5
Polyacrylamide (PAM)	base polymer	5-7%	5-7%	14 – 21
Polyethyleneimine (PEI)	crosslinker	0-1.25%	0-1.25%	0 – 5

Table 3.2: Experimental matrix

PAM/PEI	0.5%	0.75%	1%	1.25%
6%	-	√	√	√
7%	√	√	√	-

3.3.3 Filtration Testing

Sealing experiments were conducted with a Permeability Plugging Testing (PPT) apparatus under static conditions. The PPT apparatus is equipped with the tapered 3D printed disc, as shown in Figure 3.8. This unique orientation on the disc mimics drilling-induced fractures in downhole conditions. This material offers more flexibility than conventional aluminum discs in terms of design.

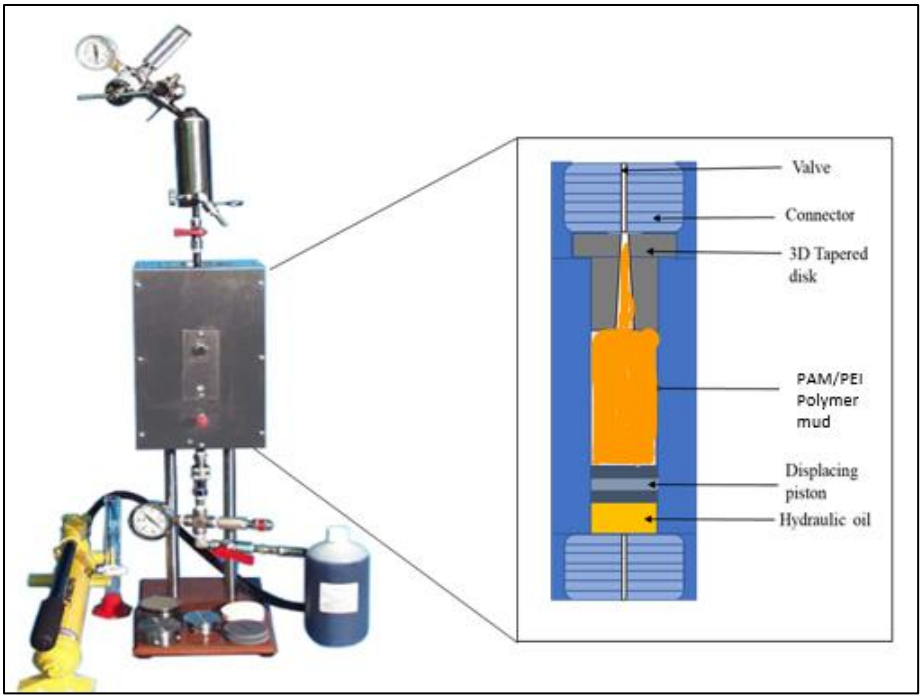

Figure 3.8: Schematic of PPT with 3D tapered fracture disc

The fluid used in this test is a water-based mud compounded by a high-pressure, high-temperature (HPHT) polymer that provides the rheology necessary for keeping the SMP in suspension under static conditions. The HPHT polymer is heated up to 300°F for at least 30 minutes for activation. Then the fluid is cooled down to room temperature to add the SMP. With this preparation, the sample is ready for the PPT tests. It is important to note that the only solids in the fluid sample are the SMP. In this case, the SMP and crosslinked PAM/PEI polymer mud only perform the bridging and sealing process.

The filtration tests were conducted by applying a pressure of 800 psi at 200°F for 30 minutes. The spurt loss filtrates and cumulative filtrates after 7.5 minutes and 30 minutes were recorded. The sealing pressure across the fracture face was also noted.

3.3.4 Alkalinity Tests

The polymer mud gel's hydrogen ion concentration (pH) determines how acidic or basic the polymer mud gel is. The pH value is measured using a PH700 Benchtop pH meter. Figure 3.9 shows the pH meter used in this study. The effects of PAM and PEI concentration on the pH value of the polymer mud is investigated.

Figure 3.9: PH700 Benchtop pH meter.

Chapter 4 : Results & Discussion

This chapter presents the results of all the experiments conducted in this study. The first part involves optimizing shape memory polymer (SMP) to minimize the fluid loss in large complex fractures. The particle size distribution of SMP is considered and compared with a conventional lost circulation material (LCM), walnut. Then the results of the sealing test are presented. We conclude the first case study with the data analysis of the experimental results. The second half of the study includes the optimization of settable crosslinked polymers for sealing complex tapered fractures. The rheology investigation is discussed, and the sealing tested is compared to the SMP and based mud.

4.1 Shape Memory Polymer (SMP)

4.1.1 Particle Size Distribution (PSD) Analysis

Figure 4.1 shows the PSD of the SMP and walnut LCM samples. The mean particle diameters for SMP and walnut LCM are 1250 μm and 1000 μm, respectively. The large mean particle sizes of the SMP make them effective in plugging larger fracture openings in geothermal formations. Also, the SMP will expand as the temperature of the well increases with depth, unlike walnut LCM, which has no expanding capabilities.

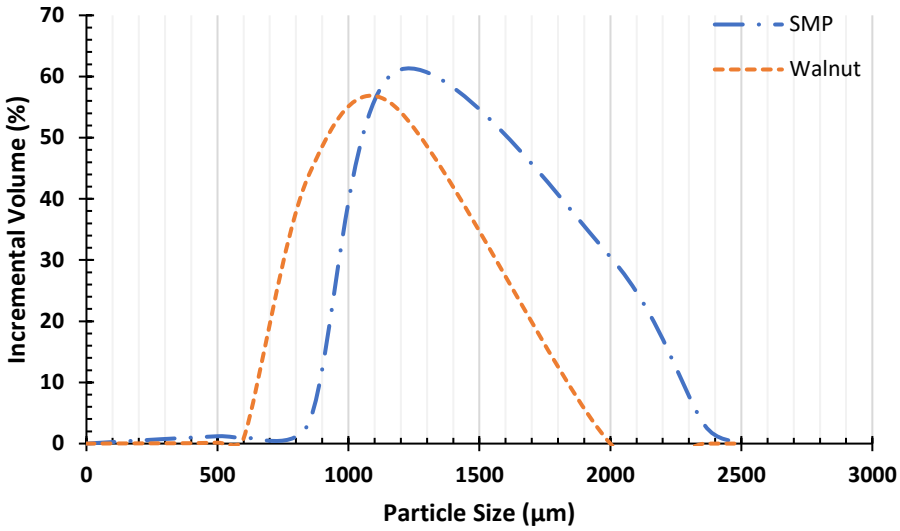

Figure 4.1: Particle size distribution for Shape Memory Polymer (SMP) and walnut LCM.

4.1.2 Fracture Sealing Test for SMP

First, we began testing at 1% SMP concentration by weight. As a result, we obtained an average cumulative filtration of 82.5 cc after 30 minutes (Figure 4.2). At this point, it is essential to note that the size of the fracture is larger, with a surface area of 100 $mm^{2,}$ and more complex than the fractures regularly tested in aluminum discs. Then, the concentration of SMP was increased to 2% by weight. In comparison to the first test, the filtration was reduced by 24.5% in the second test. Afterward, three additional tests with an SMP concentration of 3%, 4%, and 5% were performed. The increase in SMP concentration showed an effective reduction in the filtration volume. With 3% SMP, the 30-minute filtration recorder was 40 cc (51.5% reduction compared with the initial test). With 4% of SMP, the 30-minute cumulative filtration recorded was 41 cc (50.4% reduction from the initial test). The weight of the SMP was finally increased to 5%, and the average cumulative 30-minute filtration recorded is 38 cc. Thus, the reduction in the filtrate's loss has become marginal. At this point, the increase in SMP concentration is probably reaching its optimum efficiency percentage. Therefore, additional increases in this material have a less apparent effect on filtration reduction.

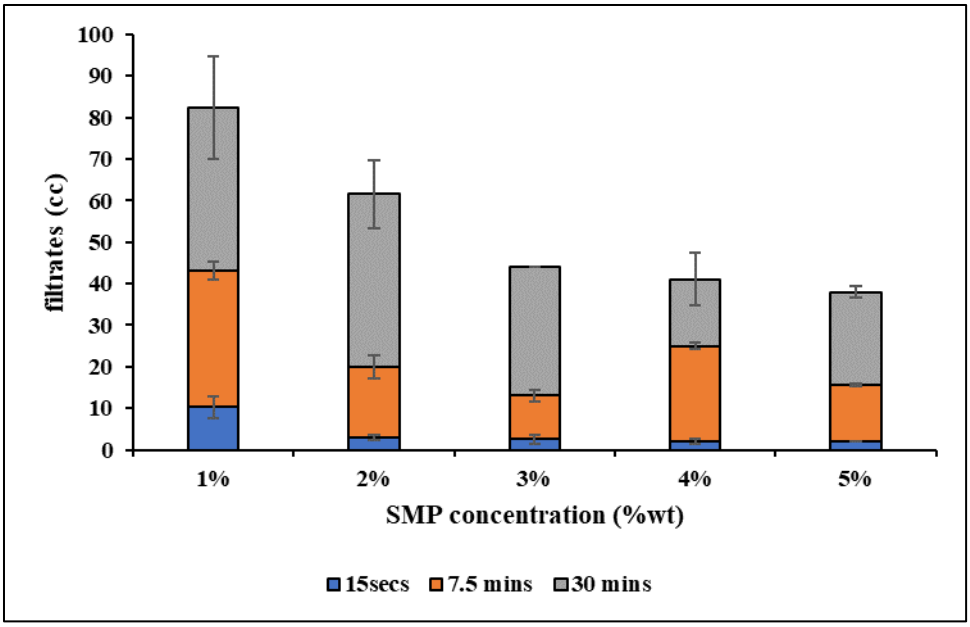

Figure 4.2: Filtrate losses for each concentration of SMP from the PPT experiment.

The filtrates were collected incrementally at 15 seconds (spurt loss), 7.5 minutes, and 30 minutes. During the experiment, the pressure was held at 800 psi. Figure 4.2 shows the cumulative filtrate volume collected—the spurt loss for the 1% wt. SMP was 9 cc, translating to a significant loss and failure of the SMP to bridge the seal. As the SMP concentration was increased, the spurt loss was vastly reduced to between 1 and 2 cc for higher concentrations. About half of the filtrates collected after 7.5 minutes were collected at 30 minutes, excluding 4 wt% SMP. At 5% SMP, we collected the lowest cumulative filtrate loss at 38 cc after 30 minutes. This lower volume indicates that the SMP did seal the fracture.

After all the filtrate has been collected, the sealing pressure is the maximum pressure the seal can withstand without failing. Figure 4.3 shows the sealing pressure obtained for various SMP concentrations. The values recorded were stable for 30 minutes after bridging the opening. Increasing the SMP from 1% to 5% represented an increment of sealing pressure from 200 psi to 750 psi, a 275% increase in the sealing pressure.

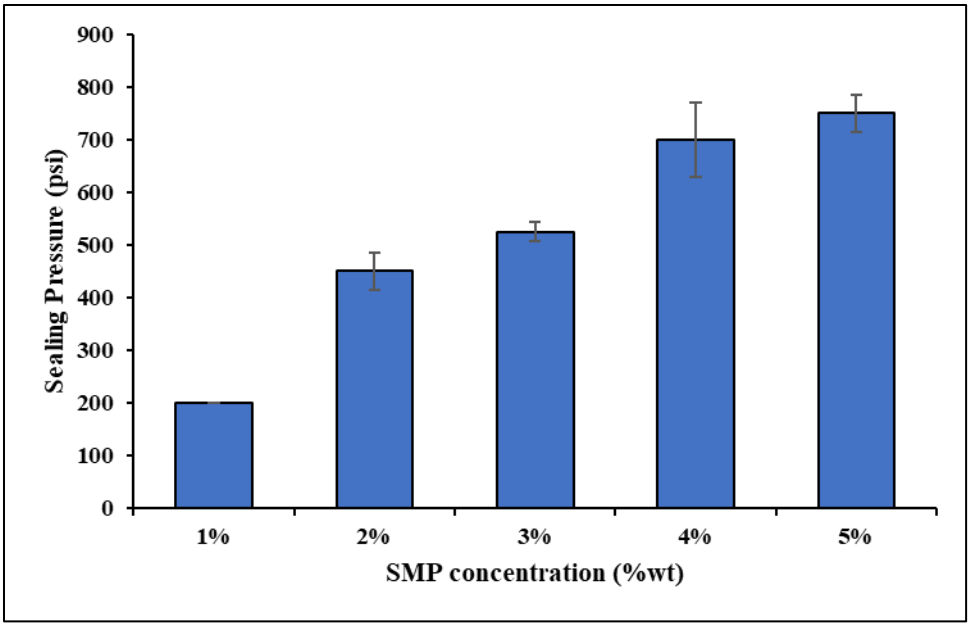

Figure 4.3: Sealing pressure for various concentrations of SMP.

The maximum sealing pressure obtained during the sealing experiment for the varied SMP concentration is presented in the plot in Figure 4.3. As observed, the increase in sealing pressure is steep as we increase the SMP concentration from 1 to 5%. This experimental data suggests that the optimal concentration of SMP for this fracture size should be around 4% and 5%.

To depict the relevancy of the results, Figure 4.4 shows the complexity of the fracture design. The combination of multiple fractures with irregular shapes and variable openings shows the versatility of the SMP in sealing various fractures. At 3% SMP concentration, we see the partial sealing of the fractures. However, at 5% SMP concentration, we see a complete sealing of the fractures. Inside the fractures, the SMP adapts to the shape variations, making this material capable of generating the bridge. This capability is essential to seal a fracture successfully. As the fractures found in geothermal reservoirs are complex networks of fractures, the adaptability demonstrated by the SMP makes this material suitable for this application.

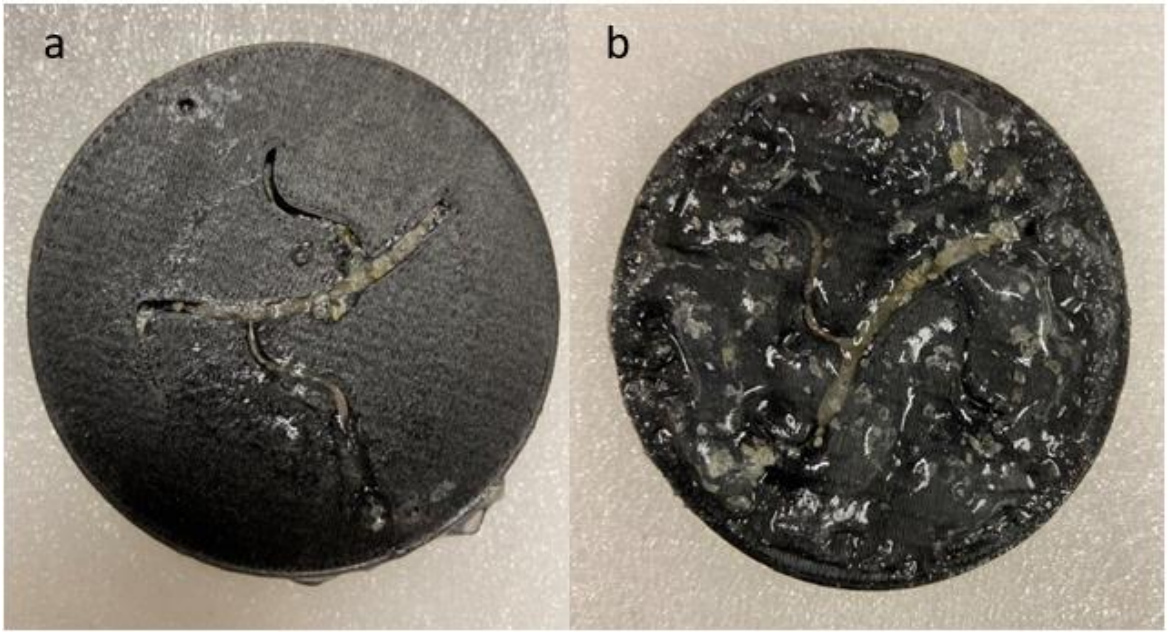

Figure 4.4: (a) Partial sealing of fractures with 3% SMP and (b) complete sealing of fractures with 5% SMP

This experimental study explores innovative ways to evaluate the filtration capability of LCMs. Using a solids-free mud ensures that the SMP only performs the sealing action. Typically, the additional solids in the drilling fluid, especially the fine particles, are expected to improve the sealing action. Also, the combination of high temperature and the complex fracture design makes this novel experimental approach relevant for geothermal research.

Figure 4.5 shows the data analysis of the maximum sealing pressure and 30 minutes cumulative filtration for various concentrations of SMP. By plotting the data points and observing the trend, it is seen that the sealing pressure increases with an increase in SMP concentration. At the same time, the cumulative filtration decreases with a power distribution as the concentration of the SMP increases.

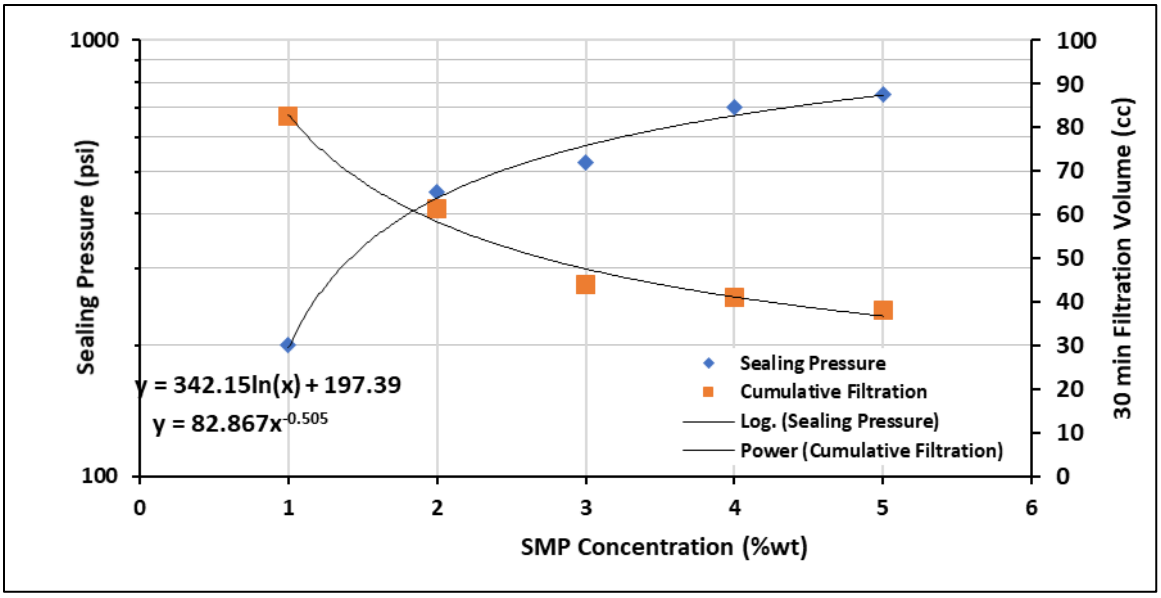

Figure 4.5: Data analysis of the maximum sealing pressure and 30 minutes cumulative filtration for various concentrations of SMP.

As seen in Figure 4.5, using the equation derived from the experimental data, if we calculate the increase in SMP concentration, the trend suggests an increase in SMP from 5% to 6% could potentially reduce filtration volume from 38 to 35.8 cc, and increase sealing pressure from 750 to 810 psi. Based upon this reasoning, the possible increase in SMP concentration led to a 6% decrease in filtration volume and an 8% increase in sealing pressure. These benefits are not enough incentives to justify the cost of the SMP, which grows astronomically for a significant fluid loss in a geothermal well. The benefits of increasing the SMP concentration even further, as high as 7% and 8%, are not apparent based on the experimental data.

4.1.3 SMP vs. Walnut

To understand how particle size distribution affects fluid loss, 5 wt% of walnut is prepared in the water-based mud (WBM) and tested using a PPT. The filtrate loss and sealing pressure of walnut are compared to those of 5 % SMP, as shown in Figures 4.2 and 4.3. The cumulative filtrate loss and sealing pressure at 5 wt% walnut is 62 cc and 500 psi, while at 5 wt% SMP, 38 cc fluid loss is recorded, and the sealing pressure is 750 psi. This improvement translates to a 39 % reduction

in fluid loss and a 50% increase in sealing pressure. Observations from Figure 4.1 shows SMP with large PSD when compared to walnut. Conclusively, SMP performed better than walnut for the same weight concentration. In operational terms, addressing lost circulation with the more expensive SMP saves drilling time. On the other hand, some operator might only consider using SMP when conventional LCMs like walnut fails to address the fluid loss problem (Lowry et al.,2022; Winn et al., 2023).

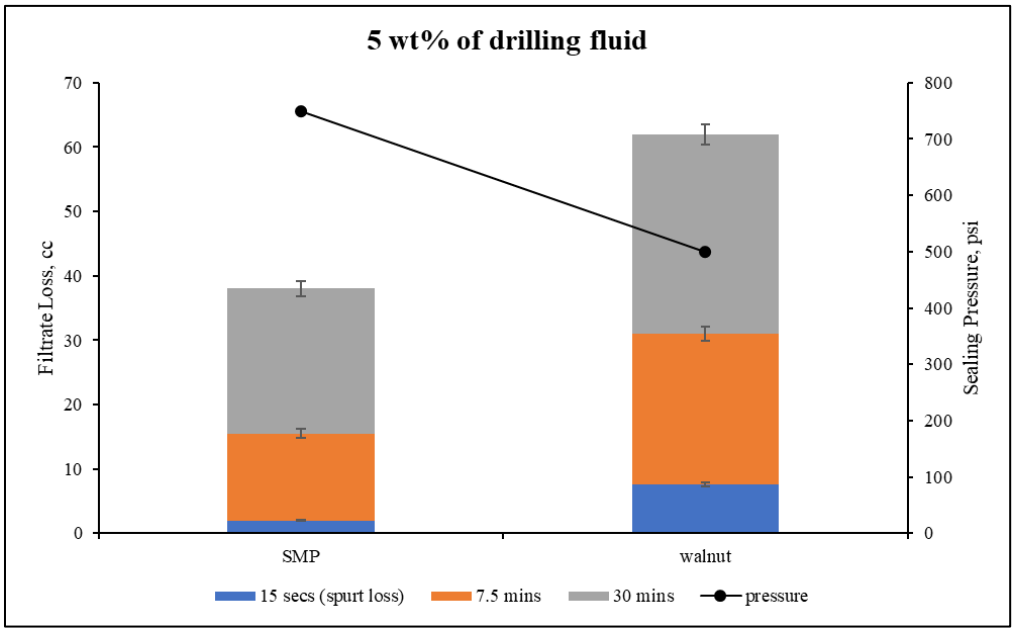

Figure 4.6: Performance of SMP and walnut at 5 wt% of drilling fluid

4.2 Settable Crosslinked Polymer Systems

4.2.1 The viscosity of gelling solutions

The PAM/PEI mud system was prepared following the procedures outlined in the methodology. Two different PAM systems with 6 and 7 wt% concentrations were prepared with distilled water. Its viscosity was measured at 150°C as a function of the shear rate. The data from the different concentrations are shown below. From Figures 4.7 and 4.8, we observed that solutions with higher concentrations of PEI had higher viscosities at any shear rate and irrespective of the absolution

concentration of the PAM than solutions with lower concentrations of PEI. This trend indicates that the crosslinking agent (PEI) concentration significantly contributed to higher viscosities in this system. In addition, the gel's viscosity reduces with increasing shear rates, indicative of a shear-thinning fluid (Bingham pseudoplastic).

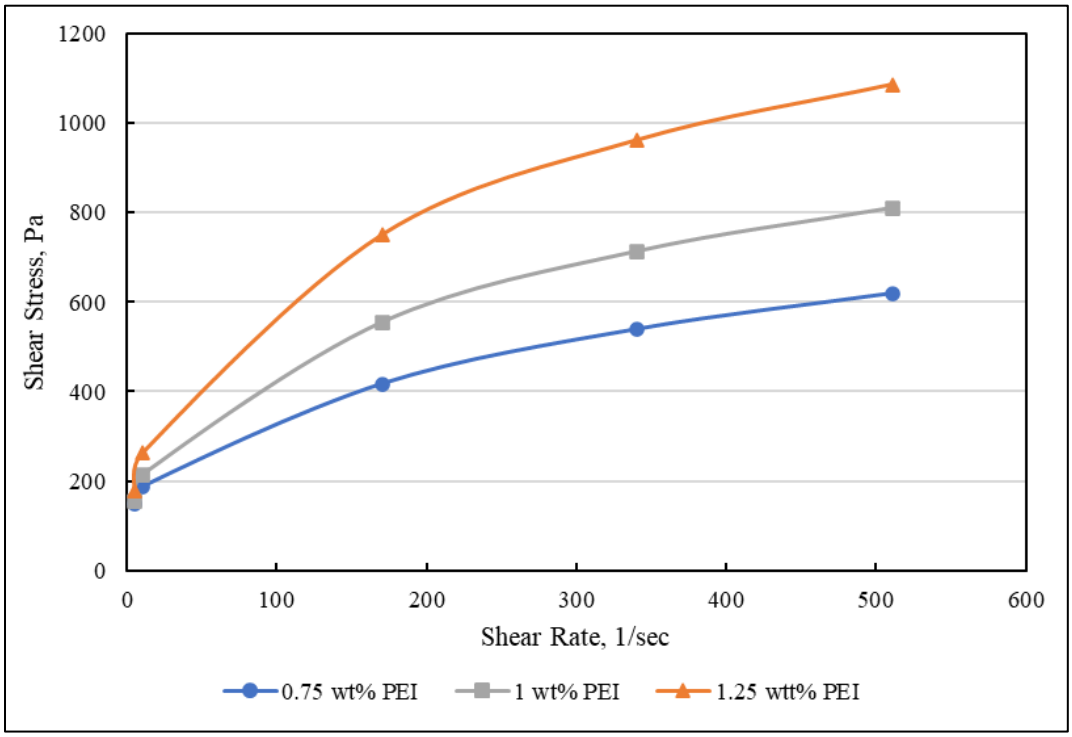

Figure 4.7: Shear stress vs. shear rate at 6 wt% PAM with varying PEI concentrations.

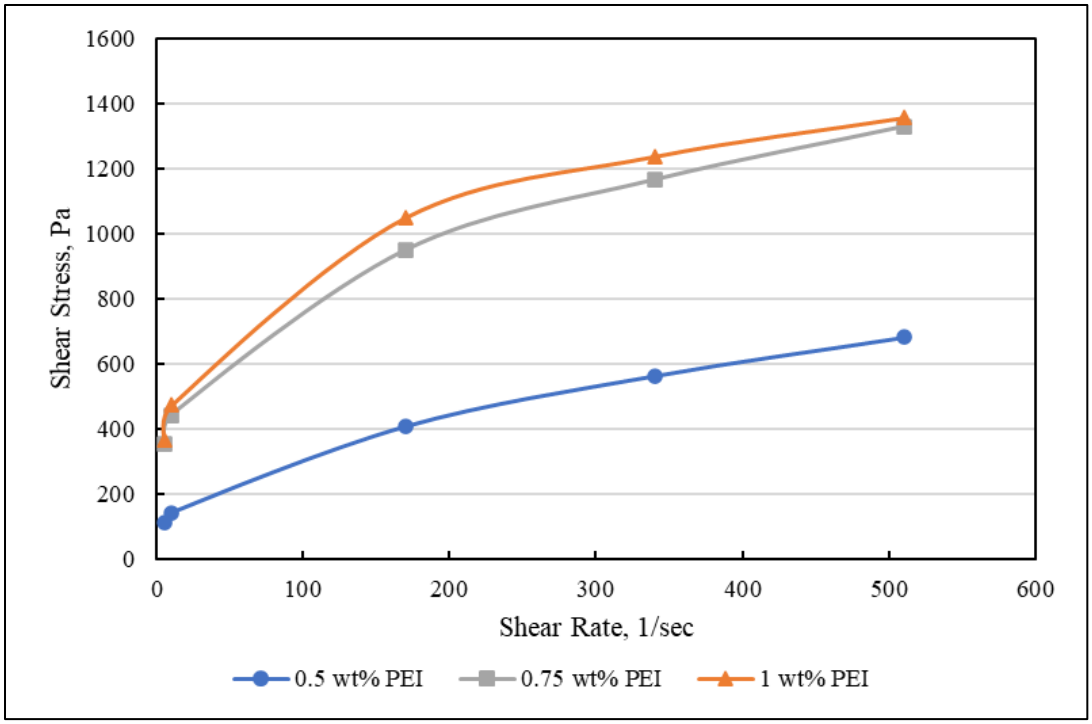

Figure 4.8:Shear stress vs. shear rate at 7 wt% PAM with varying PEI concentrations.

4.2.2 Rheology of crosslinked PAM/PEI polymer system

The polymer concentration is one of the critical parameters that provide the gel structure of the polymer mud. The effect of the polymer concentration on gelation time and the effectiveness of the polymer mud is often significant. As the polymer concentration increases, there is more crosslinking between the clay particles and the polymer. The gel formation exponentially increases, thus reducing the gelation time (Jiang et al., 2019). The viscosity versus time curve is used to optimize the concentration of the crosslinker and polymer to reveal insights into the interaction between PAM, PEI, and clay particles while observing how their interactions affect the gelation kinetics. The higher the polymer and crosslinker concentration, the more accelerated the gelation process is due to more interactions between long-chain molecular polymers (Magzoub, 2021). An abrupt increase in the viscosity indicates the onset of gelation in the polymer gel mud. The gelation rate is controlled chiefly by the polymers' concentration, crosslinker, and temperature. A retarder is required to extend the gelation time, and an accelerator is to reduce the gelation time.

The gel becomes almost solid when there is excess crosslinking of the polymer molecules, resulting in syneresis. Syneresis, or gel breakdown, is often caused by hydrolysis, the polymer's thermal degradation, and the crosslinked chain breakage. At high temperatures, multiple studies have shown that polymers containing higher concentrations of crosslinkers are susceptible to degradation and hydrolysis (Seright et al., 2021; Guo et al., 2022). We identify the occurrence of syneresis in the polymer gel mud with a distinctive viscosity signature at higher temperatures on the viscosity versus time curve.

For 7 wt% PAM polymer mud, the crosslinker concentration varied between 0.5 wt% and 1.25 wt%. Figure 4.9 shows the viscosity curve of the 7% PAM mud system at varying PEI concentrations. The onset of gelation is observed at 17, 15, and 14 minutes as the PEI concentration increases from 0.5, 0.75, and 1 wt%, respectively. For 0.5 PEI wt%, there is a gradual increase in viscosity with time. This behavior indicates sufficient bonding between the crosslinking and polymer molecules. The maximum viscosity obtained is 4.86 Pa.s. At the 1% PEI, the gelation time is 15 minutes, which is 2 minutes faster than the gelation time at 0.75 % PEI. Also, we notice the gelation rate is higher than 0.75 wt% PEI. These observations support the premise that the more the crosslinker concentration increases, the faster the onset of gelation and the higher the gelation rate. At 80 minutes into the viscosity profile, we observe the distinctive signature indicating thermal degradation and syneresis occurrence. This phenomenon is also present for the 7 wt% PAM and 1 wt% PEI gel mud.

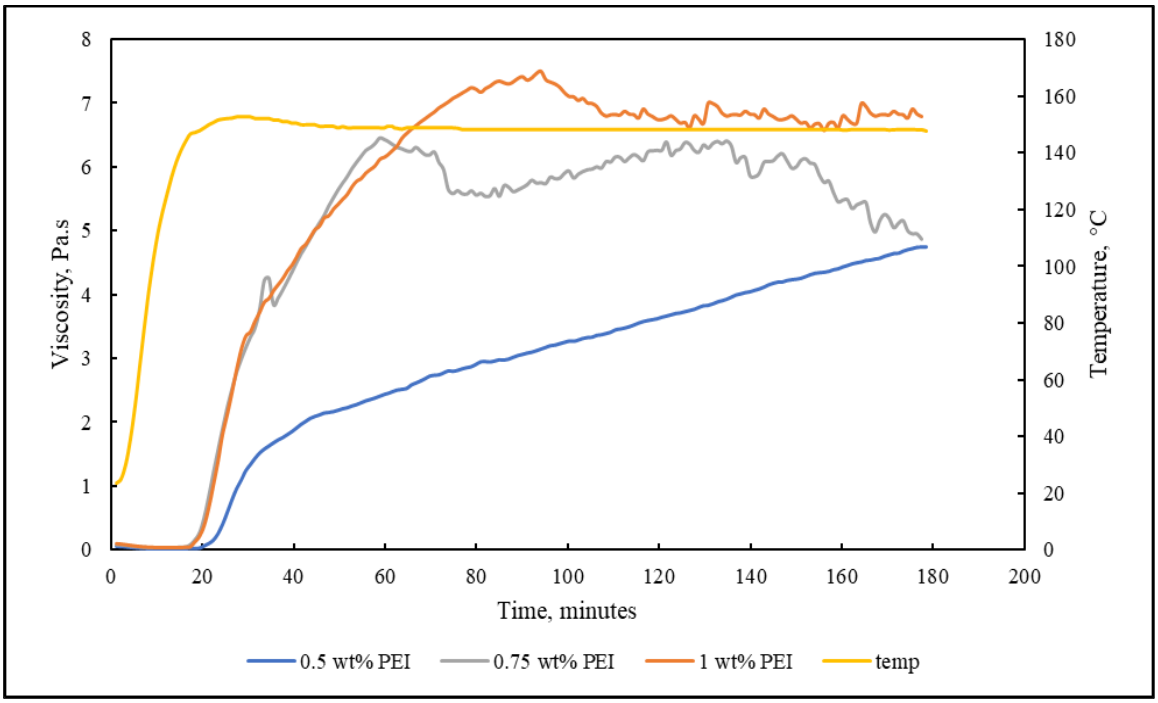

Figure 4.9: Viscosity profile for 7% PAM mud system at varying PEI concentrations at 150°C

At 6 wt% PAM, the PEI concentration varies from 0.75 wt% to 1.25 wt%. Figure 4.10 shows the viscosity curve of the 6% PAM mud system at varying PEI concentrations at 150°C (302°F). The onset of gelation is observed at 23, 17, and 16 minutes as the PEI concentration increases from 0.75, 1, and 1.25 wt%, respectively. For 0.75 wt% PEI, viscosity gradually increases with time, reaching a maximum viscosity at 7.07 Pa.s at the 3-hour mark. Increasing the PEI concentration to 1%, we observe more crosslinking between the PAM and PEI molecules. The gelation rate is noticeably higher than the gel mud with 0.75% PEI. The higher gelation rate indicates that more PAM molecules can bond and form longer chains with the PEI molecules. The maximum viscosity reached is 8 Pa.s. Finally, we increased the PEI concentration to 1.25%. The gelation time is 16 minutes, and the gelation rate is steeper. The maximum viscosity reached is 8.9 Pa.s. This optimum appears to be enough concentration to provide enough gel strength to withstand lost circulation pressures and reduce fluid loss in complex fracture networks.

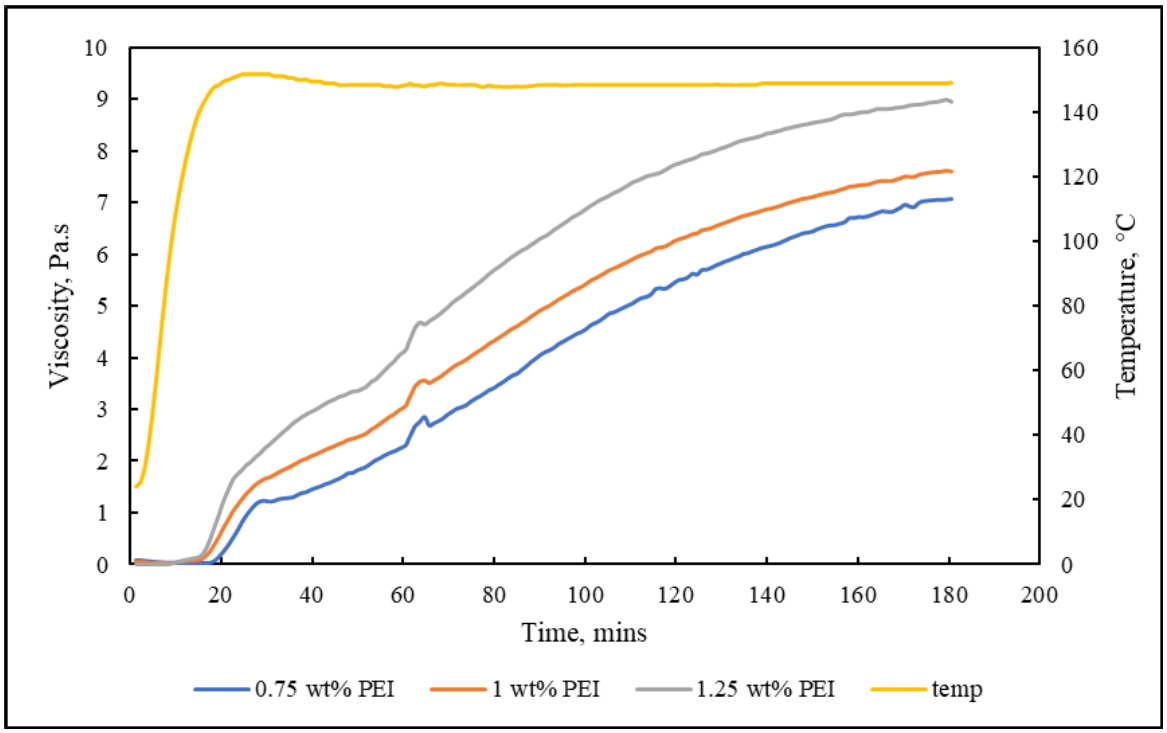

Figure 4.10: Viscosity profile for 6% PAM mud system at varying PEI concentrations at 150°C

4.2.3 Effect of PAM concentration on mud rheology and gelation

To investigate the effect of PAM concentration on the polymer mud rheology and gelation, the crosslinker concentration is held constant at 1 wt%, and the PAM concentration is varied between 5, 6, and 7 wt%. Figure 4.11 shows the viscosity curve of the 1 wt% PEI mud system at varying PAM concentrations. The gelation time decreases marginally as the PAM concentration increases from 5 to 7 wt%. The gelation rate at 7 wt% PAM is accelerated, and the polymer mud hydrolyzes rapidly at the hour mark. The reverse behavior is observed at 5 wt% PAM. The gelation rate is slower, and the polymer mud hydrolyzes after two hours. Optimum gelation is observed at 6 wt% PAM. The gelation rate is reasonably uniform, and the gel mud does not hydrolyze during the 3 hours of testing.

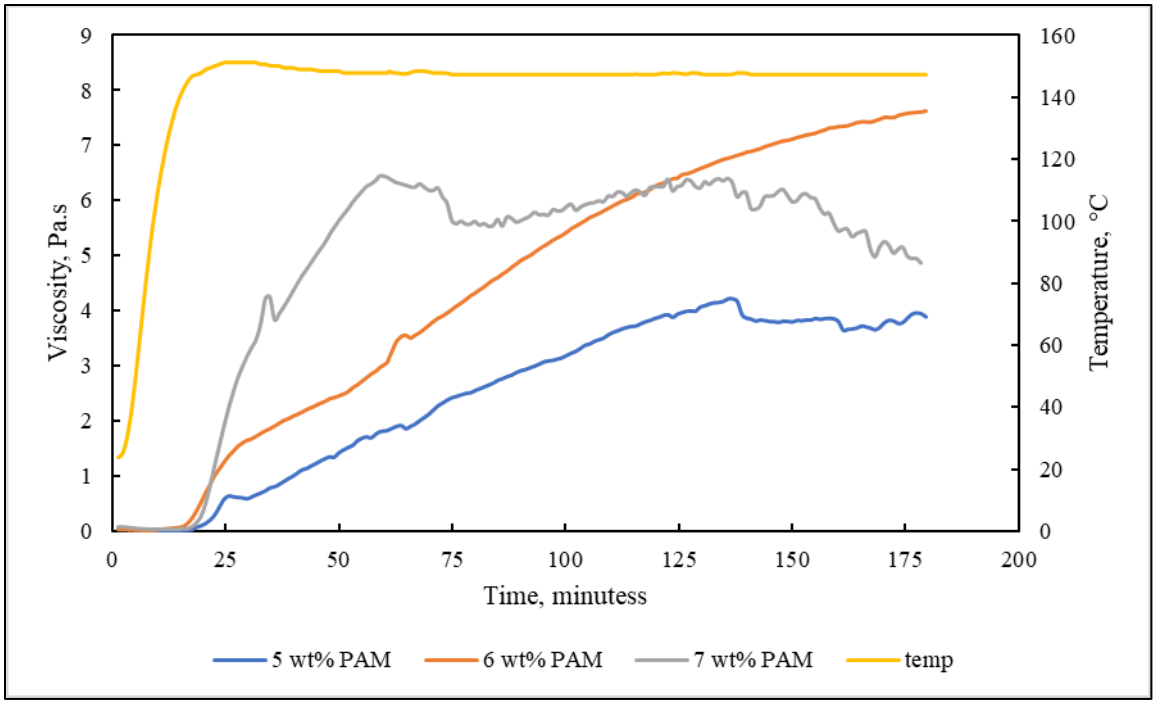

Figure 4.11: Viscosity profile for 1% PEI mud system at varying PAM concentrations at 150°C.

4.2.4 Effect of PAM concentration on initial pH

It is essential to understand the effect of PAM concentration on the initial pH of the polymer mud because the pH tends to affect the stability of polymer gel systems. With all other mud additives kept constant, the PAM concentration varied from 5– 7 wt%. After preparing the polymer mud systems, the pH was tested and ranged between 11.08 to 11.34, as shown in Figure 4.12. Increasing the polymer concentration, the pH of the total polymer mud system showed a positive correlation. After running the experiments, we also observed an average pH decrease of 0.9 points. The polymer mud's pH change correlated with the system's increasing temperature and running time. This decrease in pH appears to be due to the crosslinking reaction in the polymer mud system (Sengupta et al., 2012).

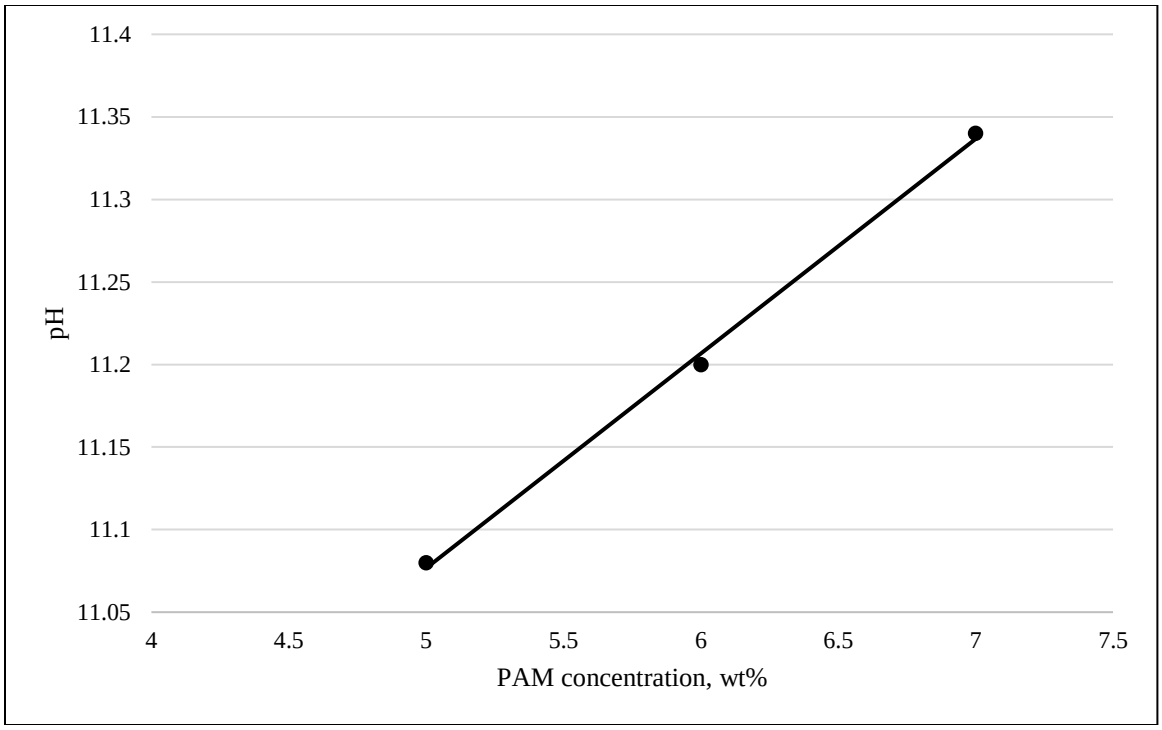

Figure 4.12: Effect of PAM concentration on initial pH

4.2.5 Fracture Sealing Test for PAM/PEI polymer system

Thermally durable LCM, such as PAM/PEI gel, can plug the leaky zones to mitigate drilling fluid loss in fractured zones while drilling in HPHT formations. This crosslinked gel could form a stable gel network capable of sealing and stopping lost circulation in fractures. Table 3.1, under Rheology Testing, shows the experimental matrix for investigating the optimum concentration of PAM and PEI for forming an efficient seal to treat mud losses. From the rheology investigated, 6% PAM and 1.25 % PEI appear to be the optimum concentration for the polymer mud. We compare the filtrate loss of the optimized mud to the base mud. The mud losses were collected at 302°F. The wait time before collecting the filtrate loss was 45 minutes to an hour, as the temperature is ramped up from room temperature of 21°C (70°F) to the desired temperature of 150°C (302°F). During the heating process, gelation starts roughly after 30 minutes, and the gel structure is formed in the PAM/PEI polymer mud, as the rheological investigation suggests.

Figure 4.13 summarizes the cumulative filtrate and maximum sealing pressure for the various test conduction. The polymeric formulation with 6% PAM and 1.25% PEI was able to seal the losses at 302°F. The cumulative filtrate loss after 30 minutes is 12 cc, and the sealing was recorded at 1500 psi. However, the base mud showed lower performance in stopping the losses at that elevated temperature, with the cumulative filtrate loss at 60 cc and sealing pressure only at 500 psi. The polymer mud reduced losses by up to 80% and improved the sealing pressure by 67%. This difference shows the ability of the crosslinked polymer mud to form a seal and prevent further losses in the formation.

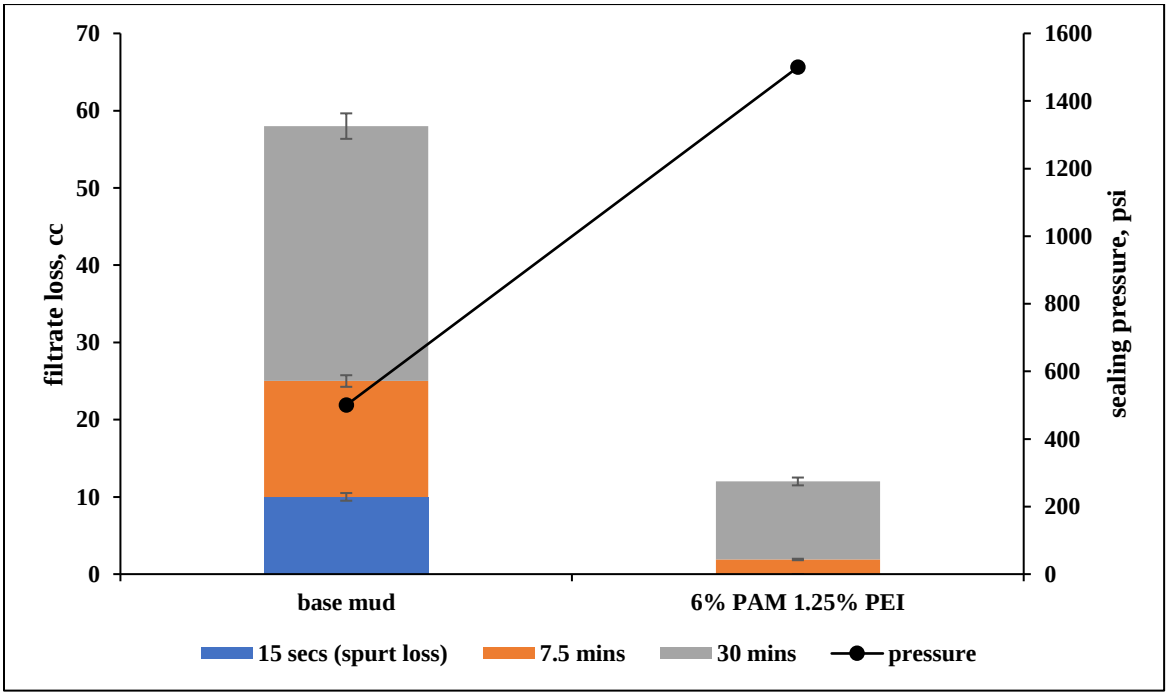

Figure 4.13: Summary of filtrate loss and sealing pressure from fracture sealing experiment

To depict the ability of the polymer mud to seal the tapered fracture totally, Figure 4.14 shows the sealed tapered fracture after the sealing experiment at (150°C) 302°F. During the drilling of formations at high temperatures, drilling-induced fractures resembling the tapered fracture designed in this study can occur. The optimized settable polymer mud with the base polymer PAM

and the crosslinker PEI can form a strong bond and seal the fractures, thereby stopping further losses into the formation.

Figure 4.14: Sealed tapered fracture with PAM/PEI polymer mud at 150°C (302°F)

Chapter 5 : Summary, Conclusion, and Recommendations

5.1 Summary

This research addresses fluid losses in high-temperature environments and the application of additive manufacturing (3D printing) in testing lost circulation material (LCM). 3D printed discs in the fracture sealing experiment allow for more realistic fracture orientation. The opportunities realized from 3D printed discs include reproducibility, rapid prototyping of ideas from models to the specimen, and the ability to control experimental parameters that would otherwise not be possible with metal fracture discs. Two lost circulation materials are considered: shape memory polymer (SMP) and PAM/PEI polymer gel mud. Both LCMs are optimized for plugging large fractures, and the sealing potential is investigated.

5.2 Conclusion

The following conclusions were drawn based on the results and findings of this study:

- SMP showed the potential to plug large fractures in high-temperature geothermal environments. In this study, we tested the polymers at 200°F and a fracture area of 100 mm^2.
- The sealing was low at a lower concentration of SMP (1% and 2%), and the fluid loss was high. However, we see a partial sealing at 3% SMP. Complete sealing was achieved at 5% SMP.
- Sealing pressure at higher concentrations of SMP (4% and 5%) was significantly higher than at lower concentrations of SMP. This pressure indicates the maximum pressure the sealed fracture face can withstand before reopening.

- The sealing pressure increases as we increase the concentration of the SMP. However, at higher concentrations (> 5%), the increase in sealing pressure is marginal and does not justify the economic cost incurred.
- The decrease in cumulative filtration follows a power distribution as we increase the concentration of the SMP. At higher concentrations (>5%), this decrease in cumulative filtration becomes marginal and does not justify the economic cost incurred.
- Also, as we increase the SMP concentration, we see that the sealing and plugging efficiency of the SMP increase likewise. However, because of the cost and rheology constraint of the SMP, the concentration cannot be increased infinitely.
- The rheology of PAM and PEI is critical to understanding the potential of the polymer mud intended for loss circulation treatment. The viscosity of 7 wt% PAM mud varied from 0.5 Pa.s 7 Pa.s, while the viscosity of 6 wt% PAM mud varied from 0.5 Pa.s to 8 Pa.s
- The PAM concentration increased the polymer mud's pH by 0.15 for every wt% increase in PAM.
- The onset of gelation of the polymer mud occurred at 18 - 23 minutes for concentrations of PEI greater than 0.5%. The higher the crosslinker concentration (> 0.5 wt%), the lower the gelation time.
- The optimum concentration for the polymer mud from the fracture sealing test is 6 wt% PAM and 1.25 wt% PEI. Fluid loss is reduced by 80% compared to the base mud with no polymers.
- Over-crosslinking, phase separation, and syneresis are significant concerns at higher concentrations of crosslinkers under high temperatures.

5.3 Recommendations

Based on this research's results, discussions, and conclusions, recommendations for future work have been proffered. The recommendations include but are not limited to the following:

1. Enhance the gelation time for deeper wells; more work can be done to investigate retarding agents such as ammonium chloride, calcium, and sodium salts.
2. The effect of bentonite on the rheology and gel of crosslinked settable polymer gel. An optimization study that determines what concentration of bentonite is suitable for improving the sealing efficiency.
3. The effects of clay interactions with shape memory polymers (SMP) and crosslinked polymers.
4. Lost circulation materials, including SMP and PAM/PEI polymer gel mud, were investigated and optimized for their ability to seal large fracture openings. However, their potential to seal small fracture openings can be considered.

Nomenclature

Abbreviations

NPT	non-productive time
LCM	lost circulation material
3D	three dimensional
SMP	shape memory polymer
PAM	polyacrylamide
PEI	polyethyleneimine
PAtBA	polyacrylamide tert-butyl acrylate
ROP	rate of penetration
ECD	equivalent circulating density
MW	mud weight
AFP	annular frictional pressures
TVD	true vertical depth
FFP	formation fracture pressure
SP	surge pressure
LOT	leak-off tests
XLOT	extended leak-off tests
DFIT	diagnostics fracture injection testing

FBP	formation breakdown pressure
HPHT	high-pressure high-temperature
Micro-C	micro cellulose
CNC	computer numerical control
CAD	computer-aided design
FDM	fused deposition modeling
PSD	particle size distribution
WBMs	wellbore strengthening materials

References

1. Abdollahi J, Carlsen IM, Mjaaland S, Skalle P, Rafiei A, Zarei S. 2004. Underbalanced drilling as a tool for optimized drilling and completion contingency in fractured carbonate reservoirs. SPE/IADC paper 91579 presented at the 2004 SPE/IADC underbalanced technology conference and exhibition held in Houston, Texas, USA, October.
2. Al-Houti N, Al-Othman M, Al-Qassar K, Al-Ebrahim A, Matar K, Abdulla A. 2017. An Alternative Method for Cement Squeeze in North Kuwait: Case Study. Paper presented at the SPE/ICoTA Coiled Tubing and Well Intervention Conference and Exhibition, Houston, Texas, USA, March, https://doi.org/10.2118/184802-MS.
3. Allahvirdizadeh P, 2020. A review on geothermal wells: Well integrity issues, Journal of Cleaner Production, Vol. 275, https://doi.org/10.1016/j.jclepro.2020.124009.
4. Al-Muntasheri A G, Nasr-El-Din A H, Peters J A, Zitha P L J, 2008. Thermal decomposition and hydrolysis of polyacrylamide-co-tert-butyl acrylate. European Polymer Journal 44, 1225–1237.
5. Al-Muntasheri G.A., Nasr-El-Din H.A., Peters J.A., Zitha, P.L.J., 2006. Investigation of a High-Temperature Organic Water-Shutoff Gel: Reaction Mechanisms. SPE J. 5–6.
6. Alsaba M, Nygaard R, Hareland G, Contreras O. 2014. Review of lost circulation materials and treatments with an updated classification. AADE-14-FTCE-25 paper presented at the 2014 AADE fluids Technical Conference and Exhibition held at Houston, Texas; April 15-16.
7. Alsaba M, Nygaard R, Saasen A, Nes O.M. 2014. Lost circulation materials capability of sealing wide fractures. SPE paper 170285 presented at the SPE Deepwater Drilling and Completions Conference held in Galveston, Texas, USA; September 10-11.

8. Anyaezu, T., Vivas, C., Salehi, S., and Li, G., 2021. Investigation into Bridging and Sealing Efficiency of Shape Memory Polymers Using Novel Additive Manufacturing. GRC Transactions, 45, pp. 2137-2147.
9. Bolton RS, Hunt TM, King TR, Thompson GEK. 2009. Dramatic incidents during drilling at Wairakei geothermal field, New Zealand. Geothermics 38:40-7.
10. Bruton J.R., Ivan C.D., Heinz T.J., 2001. Lost circulation control: Evolving techniques and strategies to reduce downhole mud losses. Proc. Drill. Conf. 1, 334–342. https://doi.org/10.2118/67735-ms.
11. Bryant, S.L., Borghi, G.P., Bartosek, M., and Lockhart, T.P, 1997. Experimental Investigation on the Injectivity of Phenol-Formaldehyde/Polymer Gelants. Paper SPE 37244, presented at the 1997 SPE International Symposium on Oilfield Chemistry, Houston, TX, 18-21 February.
12. Caughron DE, Renfrow DK, Bruton JR, Ivan CD, Broussard PN, Bratton TR, William BS. 2002. Unique crosslinking pill in tandem with fracture prediction model cures circulation losses in deepwater Gulf of Mexico. IADC/SPE paper 74518 presented at the IADC/SPE Drilling Conference held in Dallas, Texas; February 26-28.
13. Cook, J., Growcock, F., Guo, Q., Hodder, M., Van Oort, E., 2011. Stabilizing the wellbore to prevent lost circulation. Oilfield Rev. 2012, 4.
14. Cooper, K. G. 2001. Rapid Prototyping Technology: Selection and Application. Marcel Dekker, Inc., New York, NY.
15. Droger N, Eliseeva K, Todd L, Ellis C, Salih O, Silko N, Fu D, Meyer A, Bermudez R. 2014. Degradable Fiber Pill for Lost Circulation in Fractured Reservoir Sections.

IADC/SPE paper 168024 presented at the IADC/SPE Drilling Conference and Exhibition held in Fort Worth, Texas, USA; March 4-6, https://doi.org/10.2118/168024-MS.

16. Dupriest FE. 2005. Fracture closure stress (FCS) and lost returns practices. SPE/IADC paper 92192 presented at the SPE/IADC Drilling Conference held in Amsterdam, The Netherlands; February 23-25.
17. Dyre, J. C., 2006. Colloquium : The glass transition and elastic models of glass-forming liquids. Reviews of Modern Physics. 78 (3): 953–972. doi:10.1103/RevModPhys.78.953. ISSN 0034-6861.
18. El-Karsani K.S., Al-Muntasheri G.A., Hussein I.A., 2013. Polymer Systems for Water Shutoff and Profile Modification: A Review Over the Last Decade. SPE J. 19, 135–149. https://doi.org/10.2118/163100-PA.
19. El-Karsani K.S.M., Al-Muntasheri G.A., Sultan A.S., Hussein I.A.. 2015. Gelation of a water-shutoff gel at high pressure and high temperature: Rheological investigation. SPE J. 20, 1103–1112. https://doi.org/10.2118/173185-PA .
20. Ezeakacha, C.P., Salehi, S., 2018. Experimental and statistical investigation of drilling fluids loss in porous media–part 1. J. Nat. Gas Sci. Eng. 51, 104–115. https://doi.org/10.1016/j.jngse.2017.12.024
21. Ezeakacha, C.P., Salehi, S., 2019. Experimental and statistical investigation of drilling fluid loss in porous media: Part 2 (Fractures). J. Nat. Gas Sci. Eng. 65, 257–266. https://doi.org/10.1016/j.jngse.2019.03.007
22. Feng Y, Gray KE, 2016. A fracture-mechanics-based model for wellbore strengthening applications. Journal of Natural Gas Science Engineering Vol. 29, 392–400. https://doi.org/10.1016/J.JNGSE.2016.01.028.

23. Finger J, Blankenship D, 2010. Handbook of Best Practices for Geothermal Drilling. Sandia Rep. (SAND2010-6048).

24. Ford S., Despeissen M. 2016. Additive manufacturing and sustainability: An exploratory study of the advantages and challenges. Journal of Cleaner Production, 137, 1573–1587.

25. Ghalambor, A., Salehi, S., Shahri, M. P., Karimi, M., 2014. Integrated Workflow for Lost Circulation Prediction. SPE International Symposium and Exhibition on Formation Damage Control. doi:10.2118/168123-ms

26. Ghriga M.A., Grassl B., Gareche M., Khodja M., Lebouachera S.E.I., Andreu N., Drouiche N. 2019. Review of recent advances in polyethyleneimine crosslinked polymer gels used for conformance control applications. Polym. Bull. https://doi.org/10.1007/s00289-019-02687-1.

27. Halverson F, Lancaster JE, O'Connor MN 1985. Sequence distribution of carboxyl groups in hydrolyzed polyacrylamide. Macromolecules; 18(6):1139–44.

28. Hamza, A., Shamlooh, M., Hussein, I.A., Nasser, M., Salehi, S., 2019. Polymeric formulations used for loss circulation materials and wellbore strengthening applications in oil and gas wells: A review. J. Pet. Sci. Eng. 180, 197–214. https://doi.org/10.1016/j.petrol.2019.05.022

29. Hardy M, Botermans W, Hamouda A, Valdal J, Warren J, 1999. The First Carbonate Field Application of a New Organically Crosslinked Water Shutoff Polymer System. Paper SPE 50738, prepared for presentation at the 1999 SPE International Symposium on Oilfield Chemistry held in Houston, Texas, 16–19 February.

30. Harris O.O, Osisanya S.O, 2005. Evaluation of Equivalent Circulating Density of Drilling Fluids Under High-Pressure/High-Temperature Conditions. SPE Paper 97018 prepared for

presentation at the 2005 SPE Annual Technical Conference and Exhibition held in Dallas, Texas, U.S.A., 9–12 October.

31. Imrie, Andrew. 2017. Industry Applications for Additive Manufacturing. Proceedings: Offshore Technology Conference, Houston, TX.
32. Jayakumar S, Lane R H, 2012. Delayed Crosslink Polymer Flowing Gel System for Water Shutoff in Conventional and Unconventional Oil and Gas Reservoirs. Paper SPE 151699 presented at the SPE International Symposium and Exhibition on Formation Damage Control held in Lafayette, Louisiana, USA, 15–17 February.
33. Jiang, C., Zhao, G. F., Gao, M. Z., Zao, Y. X. 2016. A trial of 3D printing on rock dynamics. Proceedings: ISRM 2nd International Conference on Rock Dynamics, Suzhou, China, ISRM-ROCDYN-2016-14.
34. Khalifeh, M., Klungtvedt, K. R., Vasshus, J. K., Arild S., 2019. Drilling Fluids - Lost Circulation Treatment. Paper presented at the SPE Norway One Day Seminar, Bergen, Norway. doi: https://doi.org/10.2118/195609-MS
35. Kiran R, Teodoriu C, Dadmohammadi Y, Nygaard R, Wood D, Mokhtari M, Salehi S. 2017. Identification and evaluation of well integrity and causes of failure of well integrity barriers (A review). Journal of Natural Gas Science and Engineering 45: 511–526.
36. Lavrov, A., 2016. Lost Circulation: Mechanisms and Solutions. Gulf Professional Publishing, ISBN: 978-0-12-803916-8.
37. Li G. 2014. Self-healing composites: shape memory polymer-based structures. Wiley, West Sussex.

38. Li G., Xu W., 2011. Thermomechanical behavior of thermoset shape memory polymer programmed by cold compression: testing and constitutive modeling. J. Mech. Phys. Solids 59 (6), 1231–1250.

39. Lowry, T., Winn, C., Dobson, P., Samuel, A., Kneafsey, T., Bauer, S., Ulrich, C., 2022. Examining the Monetary and Time Costs of Lost Circulation. Stanford University, Stanford, California. Proceedings, 47th Workshop on Geothermal Reservoir Engineering. https://pangea.stanford.edu/ERE/db/GeoConf/papers/SGW/2022/Lowry.pdf

40. Magzoub M, Anyaezu T, Salehi S, Li G, Fan J, Teodoriu C, Saleh FK, Taleghani AD, 2021. Evaluating sealability of blended smart polymer and fiber additive for geothermal drilling with the effect of fracture opening size. J. Pet. Sci. Eng. 206, 108998. https://doi.org/10.1016/j.petrol.2021.108998.

41. Magzoub, M. I, Shamlooh M, Salehi S, Hussein I, Nasser M, 2021. Gelation kinetics of PAM/PEI-based drilling mud for lost circulation applications. Journal of Petroleum Science and Engineering 200, 108383.

42. Magzoub, M., Salehi, S., Li, G., Fan, J., Teodoriu, C., 2021. Loss circulation prevention in geothermal drilling by shape memory polymer. Geothermics, Volume 89, https://doi.org/10.1016/j.geothermics.2020.101943.

43. Magzoub, M.I, Salehi, S., Hussein, I., Nasser, M., 2020. Development of a Polyacrylamide-Based Mud Formulation for Loss Circulation Treatments. J. Energy Resour. Technol. 143. https://doi.org/10.1115/1.4048682

44. Magzoub, M.I., Salehi, S., Hussein, I.A., Nasser, M.S., 2020. Loss circulation in drilling and well construction: The significance of applications of crosslinked polymers in wellbore

strengthening: A review. J. Pet. Sci. Eng. 185, 106653. https://doi.org/10.1016/j.petrol.2019.106653

45. Magzoub, M.I., Salehi, S., Hussein, I.A., Nasser, M.S., 2021. Investigation of Filter Cake Evolution in Carbonate Formation Using Polymer-Based Drilling Fluid. ACS Omega 6, 6231–6239. https://doi.org/10.1021/acsomega.0c05802
46. Mannon, T., and Salehi, S. 2013. Revisiting Well Design and Formation Pressure Prediction: A Case Study from Gulf of Mexico presented at 47th US Rock Mechanics Symposium, San Francisco, June 2013.
47. Mansour A., Ezeakacha C., Taleghani A.D., Li G., Salehi S., 2017. Smart Lost Circulation Materials for Productive Zones, SPE Annual Technical Conference and Exhibition, San Antonio, Texas, USA, p. 17.
48. Mansour, A. Khaled, and A. Dahi Taleghani, 2018. Smart Loss Circulation Materials for Drilling Highly Fractured Zones. Paper presented at the SPE/IADC Middle East Drilling Technology Conference and Exhibition, Abu Dhabi, UAE, January. doi: https://doi.org/10.2118/189413-MS
49. Messenger J.U. 1981. Lost circulation, PennWell Books, p. 112.
50. Mirabbasi S M, Ameri M J, Alsaba M, Karami M, Zargarbashi A. 2022. The evolution of lost circulation prevention and mitigation based on wellbore strengthening theory: A review on experimental issues, Journal of Petroleum Science and Engineering, Volume 211, 110149, https://doi.org/10.1016/j.petrol.2022.110149.
51. Mizsei R, Li X, Chen W, Szabo M, Wang J, Wagner G, Reinherz E L, Mallis R J, 2021. A general chemical crosslinking strategy for structural analyses of weakly interacting

proteins applied to pre TCR-pMHC complexes. Journal of Biological Chemistry. 296: 100255. doi:10.1016/j.jbc.2021.100255

52. Mohamed, A., Salehi, S., Ahmed, R., Li, G., 2021. Experimental study on rheological and settling properties of shape memory polymer for fracture sealing in geothermal formations. Journal of Petroleum Science and Engineering 208: 109535. https://doi.org/10.1016/J.PETROL.2021.109535
53. Mohamed, A., Salehi, S., Ahmed, R., Li, G., 2022. Experimental study on rheological and settling properties of shape memory polymer for fracture sealing in geothermal formations. J. Pet. Sci. Eng. 208, 109535. https://doi.org/https://doi.org/10.1016/j.petrol.2021.109535
54. Moradi-Araghi A, Hsieh ET, Westerman IJ, 1988. Role of imidization in thermal hydrolysis of polyacrylamide. In: Stahl GA, Schulz DN, editors. Water soluble polymers for petroleum recovery. New York: Plenum; p. 271–8.
55. Mostafavi V., Hareland G., Aadnøy B. S., Kustamsi A, 2010. Modeling of Fracture and Collapse Initiation Gradients In Presence of Mud Cake ISRM International Symposium, Lausanne, Switzerland. ISRM-EUROCK-2010-168.
56. Obando, D., Fornasier, F., 2017. Laboratory Validation of Engineered Composite and High Fluid-Loss Materials to Help Cure Severe Losses in Fractured Formations. Paper presented at the OTC Brasil, Rio de Janeiro, Brazil. doi: https://doi.org/10.4043/28207-MS.
57. Olubode, M. O., Iradukunda, P., Karami, H., Podio, T., and McCoy, J. N., 2022a. Experimental analysis of centrifugal downhole separators in boosting artificial lift performance. Journal of Natural Gas Science and Engineering, 99, 104408. https://doi.org/10.1016/j.jngse.2022.104408

58. Olubode, M., Osorio, L., Karami, H., McCoy, J., & Podio, T., 2022b. Experimental Comparison of Two Downhole Separators in Boosting Artificial Lift Performance. In Day 1 Tue, August 23, 2022. SPE Artificial Lift Conference and Exhibition - Americas. SPE. https://doi.org/10.2118/209723-ms.
59. Palsson, B., Holmgeirsson, S., Gudmundsson, A., Boasson, H.A., Ingason, K., Sverrisson, H., Thórhallsson, S., 2014. Drilling of the well IDDP-1. Geothermics 49:23-30.
60. Park, R. G., 2005. Foundation of Structural Geology (reprint of the 1997 Chapman and Hall edition) Routledge, Abingdon, England, p. 9, ISBN 978-0-7487-5802-9
61. Petrov, Y., 2013. Structural-temporal approach to modeling of fracture dynamics in brittle media. Rock Dynamics and Applications – State of the Art. CRC Press. pp. 101–10. doi:10.1201/b14916-10. ISBN 978-1138000568.
62. Polsky Y., Armstrong K., Price C., Su J. C., Wang A., Porse, S. 2020. Study of Additive Manufacturing Application to Geothermal Technologies. Proceedings: 45th Workshop on Geothermal Reservoir Engineering, Stanford University, Stanford, CA, SGP-TR-216.
63. Prud'homme, R.K., Uhl, J.T., Poinsatte, J.P., Halverson, F, 1983. Rheological Monitoring of the Formation of Polyacrylamide/Cr+3 Gels, Soc. Petroleum Eng. Journal, 10, p804.
64. Raabe G, Jortner S. 2022. Chapter One - Well control discussion and theories, Universal Well Control, Gulf Professional Publishing, Pages 1-77, https://doi.org/10.1016/B978-0-323-90584-8.00001-0.
65. Ratna D, Karger-Kocsis J. 2008. Recent advances in shape memory polymers and composites: a review. J Mater Sci 43:254–269.

66. Reddy, B.R., Eoff, L., Dalrymple, E.D., Black, K., Brown, D., and Rietjens, M. 2003. A Natural Polymer-Based Cross-Linker System for Conformance Gel Systems. SPE J. 8 (2): 99–106. SPE-84937-PA. doi: 10.2118/84937-PA.

67. Reyes-Labarta J A, Marcilla A, Sempere J, 2011. Kinetic Study of the Thermal Processing and Pyrolysis of Crosslinked Ethylene Vinyl Acetate-Polyethylene Mixtures. Industrial & Engineering Chemistry Research. 50 (13): 7964–7976. doi:10.1021/ie200276v.

68. Rickard B, Samuel A, Spielman P, Otto M, Nickels N. 2010. Successfully Applying Micronized cellulose to Minimize Lost circulation on the PUNA Geothermal Venture Wells. GRC Transactions, Vol. 34.

69. Rickard, B., Samuel, A., Lee, C., Spielman, P., Cuadros, I., Long, J., Roberts, E., 2011. KS 14 Puna Geothermal Venture: flawless execution of aerated mud drilling with mudmotor in hostile environment. Geotherm. Resour. Counc. Trans. 35, 229–232.

70. Saleh F K, Teodoriu C, Ezeakacha C P, Salehi S. 2020. Geothermal Drilling: A Review of Drilling Challenges with Mud Design and Lost Circulation Problem. PROCEEDINGS, 45th Workshop on Geothermal Reservoir Engineering Stanford University, Stanford, California, February 10-12, SGP-TR-214.

71. Salehi S, Nygaard R. 2011. Evaluation of New Drilling Approach for Widening Operational Window: Implications for Wellbore Strengthening. Paper presented at the SPE Production and Operations Symposium, Oklahoma City, Oklahoma, USA, March, https://doi.org/10.2118/140753-MS.

72. Salehi, S., Nygaard, R., 2012. Numerical Modeling of Induced Fracture Propagation: A Novel Approach for Lost Circulation Materials (LCM) Design in Borehole Strengthening

Applications of Deep Offshore Drilling. SPE/IADC 135155, SPE Annual Technical Conference and Exhibition, October 2012, San Antonio, TX.

73. Satyam S, Arpan B, Sudipta S, Biswajit R, Dipak R, Vinod K, Aswal P M. 2017. Novel shape memory behaviour in IPDI based polyurethanes: Influence of nanoparticle, Polymer, Volume 110, 95-104, https://doi.org/10.1016/j.polymer.2016.12.080.
74. Sengupta, B., Sharma, V.P., Udayabhanu, G, 2012. Gelation studies of an organically cross-linked polyacrylamide water shut-off gel system at different temperatures and pH. J. Pet. Sci. Eng. 81, 145–150 https://doi.org/10.1016/j.petrol.2011.12.016.
75. Shamlooh M, Hamza A, Hussein I A., Nasser M S., Magzoub M, Salehi S. 2019. Investigation of the rheological properties of nano silica reinforced Polyacrylamide/Polyethyleneimine gels for wellbore strengthening at high reservoir temperatures. Energy Fuel: 33 (7), 6829–6836, https://doi.org/10.1021/acs.energyfuels.9b00974.
76. Shamlooh M., Hamza A., A. Hussein I. S., Nasser M., Salehi S., 2020. Reinforcement of Polyacrylamide-Co-Tert-Butyl Acrylate Base Gel Using Nanosilica for Conformance Control at Low and High Reservoir Temperatures. SPE Int. Conf. Exhib. Form. Damage Control. https://doi.org/10.2118/199324-MS.
77. Sharma, A., Al Dushaishi, M., R. Nygaard, 2021. Fixed Bit Rotary Drilling Failure Criteria Effect on Drilling Vibration. Paper presented at the 55th U.S. Rock Mechanics/Geomechanics Symposium, Virtual, June, ARMA-2021-2083.
78. Spielman, P., Rickard, W., Teplow, W., 2006. Puna Geothermal Venture, Hawaii—2005 drilling program. Geotherm. Resour. Counc. Trans. 30, 309–313.

79. Sveinbjornsson BM, Thorhallsson S. 2014. Drilling performance, injectivity and productivity of geothermal wells. Geothermics 50:76-84.
80. Sweatman R., Wang H., Xenakis H. 2007. Wellbore Stabilization Increases Fracture Gradients and Controls Losses/Flows During Drilling 1–15. https://doi.org/10.2523/88701-ms.
81. Tare UA, Whitfill DL, Mody FK. 2001. Drilling fluid losses and gains: case histories and practical solutions. SPE paper 71368 presented at the SPE annual technical conference and exhibition held in New Orleans, Louisiana, 30 September - 3 October.
82. Uranta G K, Rezaei-Gomari S, Russell P, Hamad F. 2018. Studying the Effectiveness of Polyacrylamide (PAM) Application in Hydrocarbon Reservoirs at Different Operational Conditions. Energies 11, no. 9: 2201. https://doi.org/10.3390/en11092201
83. Van Der Pluijm, B. A., Marshak, S., 2004. Earth Structure- Second Edition W. W. Norton & Company, Inc. New York, ISBN 0-393-92467-X.
84. van Oort E, Razavi SO. 2014. Wellbore strengthening and casing smear: the common underlying mechanism. IADC/SPE paper 168041 presented at the 2014 IADC/SPE Drilling Conference and Exhibition held in Fort Worth, Texas, USA; March 4-6.
85. Vivas C, Castillo C, Salehi S, Li G, 2022. Additively Manufactured Fracture Disk for Testing Shape Memory Polymer Based Lost Circulation Material for Geothermal Applications. GRC Transactions, 47, SGP-TR-223.
86. Vivas C, Salehi S. 2021. Rheological investigation of effect of high temperature on geothermal drilling fluids additives and lost circulation materials. Geothermics, Volume 96, 102219, ISSN 0375-6505, https://doi.org/10.1016/j.geothermics.2021.102219.

87. Vivas, C., Salehi S., 2021. Wellbore Strengthening for Geothermal Applications: Experimental Study of Thermal Degradation of LCM to Address Wellbore Tensile Failure. Paper presented at the 55th U.S. Rock Mechanics/Geomechanics Symposium, Virtual, ARMA-2021-2059.

88. Voit, W., Ware, T., Dasari, R. R., Smith, P., Danz, L., Simon, D., Barlow, S., Marder, S. R., Gall, K., 2010. High-Strain Shape-Memory Polymers. Advanced Functional Materials. 20: 162–171. doi:10.1002/adfm.200901409. S2CID 97133730.

89. Wang H., Sweatman R., Engelman B., Deeg W., Whitfill D., Soliman M., Towler, B. 2005. Best Practice in Understanding and Managing Lost Circulation Challenges. Paper SPE 95895 presented at the SPE Annual Technical Conference and Exhibition held in Dallas, Texas, 9-12 October.

90. Whitfill DL, Hemphill T. 2003. All lost-circulation materials and systems are not created equal. SPE paper 84319 presented at the SPE annual technical conference and exhibition held in Denver, Colorado, USA; 5-8 October.

91. Whitfill DL, Wang H, 2005. Making Economic Decisions to Mitigate Lost Circulation, in: SPE Annual Technical Conference and Exhibition. p. SPE-95561-MS. https://doi.org/10.2118/95561-MS.

92. Winn, C., Dobson, P., Ulrich, C., Kneafsey, T., Lowry, T. S., Akerley, J., Delwiche, B., Samuel, A., & Bauer, S., 2023. Context and mitigation of lost circulation during geothermal drilling in diverse geologic settings. In Geothermics (Vol. 108, p. 102630). https://doi.org/10.1016/j.geothermics.2022.102630.

93. Wu Q, Ge J, Ding L, Wei K, Liu, Y, Xuefeng D. 2021. A Successful Field Application of Polymer Gel for Water Shutoff in a Fractured Tight Sandstone Reservoir. Paper presented

at the SPE Middle East Oil & Gas Show and Conference, event canceled, November, https://doi.org/10.2118/204741-MS.

94. Zhong A., Ornelaz, R., Krishnan, K. 2017. Exploration of Applications of Metallic Additive Manufacturing for the Oil and Gas Industry. Proceedings: Offshore Technology Conference, Houston, TX, 0TC-27540-MS.
95. Zhou T., Zhu, J. 2017. An Experimental Investigation of Tensile Fracturing Behavior of Natural and Artificial Rocks in Static and Dynamic Brazilian Disc Tests. Procedia Engineering, 191, 992 – 998.
96. Zhou, Lei, Li, Honglian, Ren, Xiangyan, Chen, Junchao, Cai, Jianchao. 2022. Chapter Five - Hydraulic fracturing of unconventional reservoirs aided by simulation technologies, The Fundamentals and Sustainable Advances in Natural Gas Science and Eng, Sustainable Natural Gas Reservoir and Production Engineering, Gulf Professional Publishing, Volume 1, Pages 107-141, https://doi.org/10.1016/B978-0-12-824495-1.00013-9.

Appendix A: Research Outcomes: Journals and Conference Proceedings

1. Magzoub, M., Anyaezu, T., Salehi, S., Li, G., Fan, J., Teodoriu, C., Saleh, F.K., Taleghani, A.D., 2021. Evaluating sealability of blended smart polymer and fiber additive for geothermal drilling with the effect of fracture opening size. J. Pet. Sci. Eng. 206, 108998. https://doi.org/10.1016/j.petrol.2021.108998.
2. Anyaezu, T., Vivas, C., Salehi, S., and Li, G., 2021. Investigation into Bridging and Sealing Efficiency of Shape Memory Polymers Using Novel Additive Manufacturing. GRC Transactions, 45, pp. 2137-2147.
3. Anyaezu, T., Magzoub, M., Salehi, S., 2023. Musaab. Experimental Investigation of PAM/PEI Polymer Mud for Reducing Lost Circulation in High-Temperature Formations. Geothermics (Review). http://dx.doi.org/10.2139/ssrn.4394925